Chapter 5

The LS84 Model

5.1 Understanding Climate in a Simple Atmosphere-Ocean Model

As described by Palmer (1993), and highlighted in chapter three, the L63 model evolves with two characteristic time scales: the oscillation time around the regime (or lobe) centroids, and a residence time within each regime (or lobe) of the model attractor. Similarly, the L84 model is characterised by the time spent orbiting the primary lobe of the attractor (denoting westerly motion) and the frequency of transitions to the secondary lobe (denoting easterly motion). For conventional parameter values, both systems have been shown to display transitive behaviour with regular transitions between attractor lobes. In addition, the L84 model exhibits intransitive behaviour for particular values of F (e.g. when $F = 6$). In the L63 and L84 models, the regularity of regime and lobe transitions occurring in transitive regions of parameter space ensures that the model attractors are reasonably well explored by observing single model trajectories over relatively short time scales (see sections 3.3.2 and 4.3.1). Ergodicity is therefore observed in the L63 and L84 models (in the absence of climate change and nonlinear parameter fluctuations) using relatively short single trajectory simulations, as demonstrated in the numerical experiments presented in section 3.3.3 for the L63 model and section 4.3.3 for the non-seasonally driven L84 model.

In developing the analogy to the climate system and considering the time scales of interest for climate change adaptation, it is important to acknowledge the existence of internal climate variability which can occur on long as well as short time scales. Long-term internal climate variability occurs because the climate system is sensitive to changes in subsystems (such as the ocean, cryosphere and biosphere) which evolve on very different time scales to the atmosphere. Consequently, investigation of a coupled system consisting of two components evolving on different time scales is a valuable and necessary endeavour to further develop understanding of the role of IC uncertainty in climate change prediction.

On the time scales of interest for climate change adaptation (primarily decadal to multi-decadal) one of the dominant sources of internal climate variability is the ocean (Manabe and Stouffer (1996)). Modes of variability such as El Niño Southern Oscillation (ENSO), the Pacific Decadal Oscillation (PDO) and the Atlantic Multidecadal Oscillation (AMO) are driven by the nonlinear dynamic interactions of the ocean and atmosphere which affects global and regional weather patterns (Anderson and Willebrand (1996), Ghil (2002) and Delworth et al. (2007)). Furthermore, the heat content and thermal inertia of the ocean is a key factor in determining the rate and extent of climate change. Accounting for the impact of the oceans (in addition to other slowly evolving climate drivers) on present and future climate is therefore key to the success of climate model experiments designed to aid climate change adaptation.

In this chapter, the role of IC uncertainty in climate prediction is investigated in relation to internal climate variability induced by the interaction of subsystems operating on different dynamic time scales. The obvious limitation of investigating this issue with operational GCMs, aside from model inadequacy and lack of process understanding for key modes of variability (Huang et al. (2004)), is the expense and computational demands of running large IC ensembles. Therefore, this chapter will present the theoretical case for adequately sampling IC uncertainty using a simple system considered analogous to the climate system, in the perfect model scenario (PMS).

The experiments presented in this chapter are conducted with a simple coupled model developed by Van Veen et al. (2001) (referred to as the LS84 model) combining the L84 model with the much studied Stommel-61 (S61) ocean box model. The L84 component of the coupled model evolves on a relatively fast time scale compared to the S61 model. Consequently, the L84 model is considered analogous to the atmospheric component, and the S61 model represents the more slowly evolving ocean component. The dynamic evolution of the model variables are described further in section 5.2.

In section 5.2, the LS84 model is described and the parameter transformations from the uncoupled L84 model are outlined. This section also shows the geometry of the LS84 model pseudo-attractor by illustrating a single model trajectory in the atmosphere (L84) and ocean (S61) variables. Section 5.3 details the evolution of the LS84 model climate distributions from both a single trajectory and IC ensembles for two types of atmosphere-ocean coupling referred to as "active" and "passive" coupling (described in section 5.2). The ergodic hypothesis is investigated by comparing single trajectory distributions to ensemble distributions and the time scale of convergence for model distributions is elicited. Section 5.4 investigates the use of IC ensembles to inform probabilistic assessments of the model climate. The almost intransitive[1] nature of the model (under passive coupling) is exploited to estimate the probability of transitions between model regimes. The memory of ICs is explored in section 5.5 by comparing convergence rates of model distributions for IC ensembles initiating from different regions in the pseudo-attractor state space. In section 5.6, the LS84 model is investigated when subject

[1]See definition provided in section 2.1.4 and in the glossary.

to forced transient changes in key model parameters. The behaviour of both single model trajectories and IC ensembles are explored and the results are linked to the use of the ergodic assumption in climate change projections. Finally, the results of the experiments conducted with the LS84 model are discussed in section 5.7 and are related to the issues of climate prediction, under altered forcing conditions, for a system which displays dynamic behaviour dependent on the boundary conditions.

5.2 The LS84 Model

5.2.1 Coupling L84 to the S61 model

In extending the use of simple models as analogies to the climate system, the S61 model is utilised to represent the ocean component in a simple coupled atmosphere-ocean model. As described in section 2.4.3, the S61 model was developed by Henry Stommel in 1961 to demonstrate the impact of two important ocean variables which influence sea-water density and drive the circulation of ocean currents; namely temperature and salinity (Stommel (1961)). In essence, the two-box model is a simple representation of the thermohaline circulation (THC) showing the direction and intensity of the flow governed by the temperature and density differences between two ocean "vessels". Despite its simplicity, oceanographers and climate researchers continue to study versions of the S61 model to gain insight into the THC and the dynamics of the ocean-atmosphere system (Hearn (1998), Lohmann and Scheider (1998) and Wunsch (2005)). The presence of multiple equilibria, stable (and unstable) model states and the existence of hysteresis in the S61 model have led scientists to examine the results from the model in relation to more complex GCMs (Prange et al. (2002)). Of course, in such an idealised model, there are a number of assumptions which limit the model's realism. For example, the assumption that each ocean box (or vessel) is well mixed is particularly crude as the vertical gradient in ocean temperature can be considerable, especially in the tropics (Pacanowski and Philander (1981)).

The S61 model equations used by Van Veen et al. (2001) are given in equations 5.1 to 5.3:

$$\dot{T} = k_a(T_a - T) - |f(T,S)|T - k_w T \tag{5.1}$$

$$\dot{S} = \delta - |f(T,S)|S - k_w S \tag{5.2}$$

$$f = \omega T - \epsilon S \tag{5.3}$$

where T is the equator-to-pole temperature difference ($T_e - T_p$), S is the equator-to-pole salinity difference ($S_e - S_p$) and f is the strength of the THC in sverdrups (Sv). The units for T are in degrees Kelvin (K) and the units for S are in practical salinity units (psu). When f is positive (temperature driven), the surface flow is poleward and the return (deep) flow is equatorward. When f is negative (salinity driven) the situation is reversed and the surface flow is equatorward whilst the return (deep) flow is poleward. For certain parameters, both possibilities occur as stable solutions in the S61 model (Stommel (1961)). T_a is the inhomogeneous forcing by solar heating and δ is the coefficient of atmospheric water transport. k_a is the coefficient of heat exchange between the ocean and atmosphere, k_w is the coefficient of internal diffusion and ω and ϵ derive from the linearised equation of state.

In coupling the L84 model equations (given in equations 4.1 to 4.3) to the S61 model, Van Veen et al. (2001) introduced a number of transformations, which are shown in equations 5.4 to 5.7:

$$
\begin{aligned}
F &\rightarrow F_0 + F_1 T && (5.4)\\
G &\rightarrow G_0 + G_1(T_{av} - T) && (5.5)\\
T_a &\rightarrow \gamma X && (5.6)\\
\delta &\rightarrow \delta_0 + \delta_1(Y^2 + Z^2) && (5.7)
\end{aligned}
$$

where F_0 is a reference value for the equator-to-pole temperature difference in the atmosphere, G_0 is a reference value for the land-sea temperature difference, F_1 and G_1 are the coupling parameters to the ocean and T_{av} is the mean surface temperature difference between the equatorial and polar boxes. γ is the proportionality constant between the westerly wind strength and inhomogeneous forcing by solar heating (T_a). The parameter δ_0 is the reference coefficient of the atmospheric water transport and δ_1 is a measure for the rate of water transport through the atmosphere.

The coupled LS84 model is therefore given by the following equations:

$$
\begin{aligned}
\dot{X} &= -Y^2 - Z^2 - aX + a(F_0 + F_1 T) && (5.8)\\
\dot{Y} &= XY - bXZ - Y + G_0 + G_1(T_{av} - T) && (5.9)\\
\dot{Z} &= bXY - XZ - Z && (5.10)\\
\dot{T} &= k_a(\gamma X - T) - |f(T,S)|T - k_w T && (5.11)\\
\dot{S} &= \delta_0 + \delta_1(Y^2 + Z^2) - |f(T,S)|S - k_w S && (5.12)\\
f &= \omega T - \epsilon S && (5.13)
\end{aligned}
$$

where X, Y, Z, a and b assume their definitions given in section 4.2.1. Table 5.1 shows the values of the constants used in the Van Veen et al. (2001) study, which have been adopted for the experiments conducted in this thesis. For these values, the atmosphere evolves on a time scale approximately one thousand times faster than the ocean (Roebber (1995)).

Constants	Value
G_0	1
a	0.25
b	4
T_{av}	30
γ	30
k_w	$1.8 \cdot 10^{-5}$
k_a	$1.8 \cdot 10^{-4}$
ω	$1.3 \cdot 10^{-4}$
ϵ	$1.1 \cdot 10^{-3}$
δ_0	$7.8 \cdot 10^{-7}$
δ_1	$9.6 \cdot 10^{-8}$

Table 5.1: Constants used in the LS84 model (Roebber (1995), Van Veen et al. (2001)).

In the L84 model, the seasonal variation in F is given as a sinusoid over one model year, according to equation 4.4, with a maximum in mid-winter (where the equator-to-pole temperature difference is greatest) and a minimum in mid-summer. In order to maintain the analogy to the climate system and provide continuity from the previous chapter, the version of the L84 model used in the coupled system also includes a seasonal variation in F. However, in the LS84 model F is replaced by $F_0 + F_1 T$, as shown in equation 5.4. The sinusoidal variation given by equation 4.4 is therefore imposed on the reference value F_0. Because of the continuous perturbation to F_0 by the addition of the term $F_1 T$, the behaviour of the L84 component in the coupled model is always different to the uncoupled model, for non-zero values of T.

The quantitative results and subsequent model interpretation presented in this thesis are an extension of the results presented by Van Veen et al. (2001) which focusses investigation on the system with a constant equator-to-pole temperature difference, $F_0 = 8$. Van Veen et al. (2001) demonstrate that when $F_0 = 8$ the "fast variables" (L84 variables) show intermittent behaviour which is a result of the slow-varying ocean variables continually moving the system through a series of bifurcations. It is shown in section 4.2 that intermittent behaviour is also present in the uncoupled seasonally driven L84 model, where the seasonal cycle in F induces transitions from chaotic behaviour in mid-winter to alternative types of non-chaotic behaviour in mid-summer. In this chapter, the presence of a slowly-varying ocean component which modulates the seasonal cycle in F_0 is explored to investigate the quantitative and qualitative impacts on the model behaviour and crucially, the model climate distributions.

The rationale underlying the mechanisms by which the S61 and L84 models are coupled was provided by Van Veen et al. (2001). The authors note that the LS84 model can be likened to a perturbation to the L84 model. In the study, the authors differentiate between two modes of ocean coupling referred to as "passive" and "active". The prevalent mode is controlled by the coupling parameters, F_1 and G_1. Table 5.2 provides the values for the coupling parameters used by Van Veen et al. (2001). When the passive coupling parameters are used, the ocean is observed to have little effect on the evolution of the atmospheric variables, which continues to exhibit chaotic behaviour. There is not much variability in the ocean variables and Van Veen et al. (2001) state that "the ocean basically integrates the atmospheric forcing". However, when the active coupling is used, the atmospheric variables display intermittent behaviour and the ocean is found to have a significant impact on the model dynamics. Van Veen et al. (2001) show power spectra that reveal important modes of variability, likely caused by the emergence of periodicity. The relative merits of studying each coupling regime for the purposes of this thesis are examined in sections 5.2.2 and 5.3. Crucially, the coupling parameters lead to very different model behaviour for the seasonally driven LS84 model compared to the non-seasonally driven model explored by Van Veen et al. (2001).

The rich dynamics that result from the coupling of the two models are documented in the Van Veen et al. (2001) study and this knowledge is used in the design of the experiments presented in this chapter. In a later study, Van Veen uses the Maas (1994) model to act

Parameter	Ocean State	Value
F_1	Active	0.021685
	Passive	0.02
G_1	Active	0.01
	Passive	0.01

Table 5.2: Coupling parameters used in the LS84 model (Van Veen et al. (2001)).

as the ocean component of a low-order climate model while retaining the L84 model as the atmospheric component (Van Veen (2003)). This is because the Maas (1994) model is directly formulated from the governing fluid dynamical equations; the S61 model is not based on such equations. However, the S61 model is chosen for this analysis because of the existence of transitive/intransitive behaviour when coupled to the L84 model (discussed in section 5.2.3) and the familiarity of the climate modelling community with this well studied and relatively well understood model (Pagaran (2010)).

In the next section, the pseudo-attractor (PA) of the seasonally driven LS84 model is described and illustrated. The term *pseudo-attractor* (introduced in section 4.4.2) is used rather than the term *attractor* in this chapter because the parameter F_0 is a function of time.

5.2.2 The LS84 model pseudo-attractor

Coupling the S61 model to the L84 model increases the number of dimensions from three (X, Y, Z) to five (X, Y, Z, T, S) so visualising the LS84 model's pseudo-attractor for a given set of forcings becomes more difficult. Therefore, for practical reasons, the plots in figures 5.1 and 5.2 show the atmosphere and ocean variables separately to illustrate the geometric character of the model's PA for the parameter values given in table 5.1 in both the active and passive ocean coupling regimes. The regions of state space in which the model trajectories propagate are dependent on the coupling regime. In order to determine suitable ICs to help illustrate the model PA for each coupling regime, a single model simulation is performed with initial state values informed by the results of the Van Veen et al. (2001) study.

A one hundred year model simulation is conducted with ICs $(X, Y, Z, T, S) = (1.0, 1.0, 1.0, 5.5, 1.3 \times 10^{-3})$ under both passive and active coupling conditions (beginning on January 1st in the first year). The final states of the model, given in table 5.3, are assumed to be on (or very close to) the model PA under each coupling regime so these states are used as the ICs for subsequent single model trajectory plots. As in chapter four, the fourth-order Runge-Kutta integration method is employed with a time step of $\tau = 0.01$, which is equivalent to 1.2 hours (72 minutes) given the assertion that one time unit (the damping time for the waves) is approximately five days (Lorenz (1984)).

The three-dimensional plots in figure 5.1 show the evolution of the atmospheric variables from

Variable	Active	Passive
X	1.554	1.087
Y	0.778	1.129
Z	0.459	0.635
T	4.453	3.949
S	$1.605 \cdot 10^{-3}$	$1.693 \cdot 10^{-3}$

Table 5.3: ICs used for single model simulations of the LS84 model for each coupling regime.

a single realisation of the LS84 model for both active and passive coupling parameters. Whilst the behaviour of the atmosphere is altered by the presence of the ocean, the general geometric character of the model's PA in the X, Y and Z variables is similar to that of the uncoupled L84 model when $F = 8$ (see figure 4.1, section 4.2.2). The dominant flow is still westerly with occasional chaotic transitions to easterly flow denoted by the secondary lobe. The modulated behaviour induced by the presence of the ocean is difficult to detect in figure 5.1 but the impact of the ocean on the atmosphere is further elaborated in section 5.2.5. Analysis of the model behaviour is more insightful when focusing on the behaviour of the model trajectories for each individual model variable, along with the associated climate distributions.

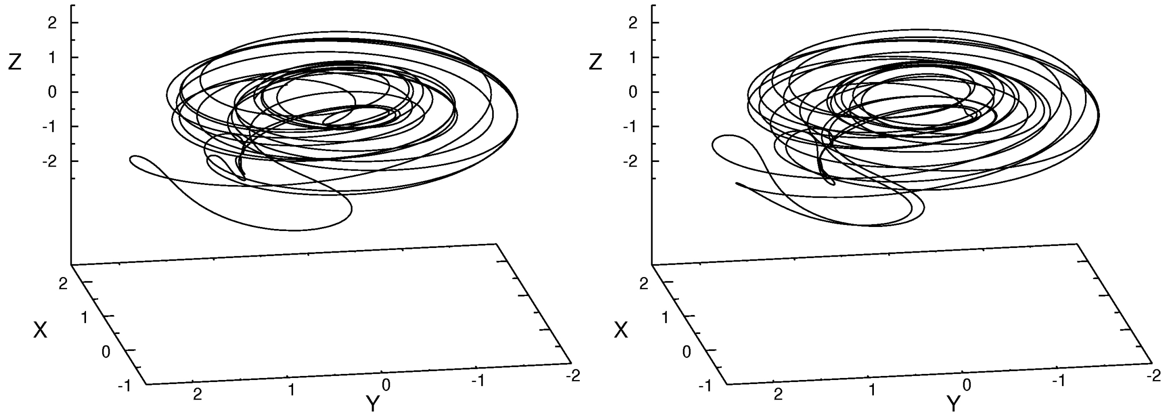

(a) Active (b) Passive

Figure 5.1: Single trajectory of the atmosphere variables from a one year simulation of the LS84 model for (a) active and (b) passive coupling parameter values. ICs given in table 5.3.

Figure 5.2 shows the evolution of the same model trajectory for the two ocean variables T and S. As the dynamic time scale of the ocean component is approximately one thousand times slower than that of the atmospheric component (Roebber (1995)), the plots show the model behaviour for considerably longer time scales, from 100 to 10,000 years. The plots in the left column of figure 5.2 show the model trajectory when subject to active coupling parameters and the plots in the right column show the model trajectory when subject to passive coupling parameters. The scale of the axes are the same for all six plots so it is therefore apparent that when the ocean is "actively" coupled to the atmosphere, the ranges in the ocean variables are more constrained in comparison to the range of behaviour in the passive coupling regime. In both regimes, it is evident that higher values of T are typically associated with lower values of S. The Pearson correlation coefficient for the data shown in figure 5.2(e) (active coupling) is $r = -0.573$ and the Pearson correlation coefficient for the data shown in figure 5.2(f) (passive coupling) is $r = -0.733$ indicating that the correlation is more significant under passive coupling.

Clearly, the PA state space is not well sampled after only 100 years of the model simulations for both coupling regimes. Even after 1,000 years, there are areas of the PA state space that have not been visited by the model trajectory. After 10,000 years, certain regions of the model state space have been visited regularly by the model trajectory but it remains unclear whether or not the PA state space has been fully explored. In section 5.3.1, the frequency distributions of the single trajectory are shown for increasing time periods for each of the ocean variables and the rates of convergence are discussed.

Of relevance to the climate analogy presented in this chapter is the emergence of two dominant regions of state space in which model trajectories oscillate, when subject to passive coupling. In figures 5.2(d) and 5.2(f), there appears to be two identifiable areas of model state space where there is a high density of data points, located at approximately $T = 4.0$ and $T = 4.4$. The emergence of *regime* behaviour suggests that the model is more stable in these regions of state space. For active coupling, regime behaviour is not evident in the plots shown in figure 5.2. Further analysis of the regime structure of the LS84 model with passive coupling is provided throughout the chapter and the implications for climate are considered in relation to known regime behaviour occurring in the climate system.

5.2.3 Single trajectory results

Van Veen et al. (2001) show that for active coupling parameters, the slow time scale of the ocean plays an important role in the ocean-atmosphere dynamics. When the model is subject to passive coupling parameters, the effect of the ocean on the coupled model dynamics is determined to be less important. However, the research presented here shows that when there is a seasonal cycle in the parameter F_0, considerable long-term internal variability can be observed in the system for passive coupling parameters while for active coupling parameters the system shows rather less variability on longer time scales. As evident in the analysis presented in this section, the coupling parameters referred to "active" and "passive" lose their previous meanings when a seasonal cycle in F_0 is introduced into the model but for continuity from the Van Veen et al. (2001) study, these terms will continue to be used throughout the analysis to denote the values of F_1 and G_1.

Figure 5.3 shows the evolution of the atmospheric variables for a period of 10 years beginning in mid-winter for both active and passive coupling. Under both modes of coupling, the behaviour of the atmospheric variables is intermittent (alternating periodic, chaotic behaviour). In the winter, when F returns to the chaotic regions of parameter space, the trajectories exhibit transitive behaviour which span the range of the model PA. In the summer, the model behaviour

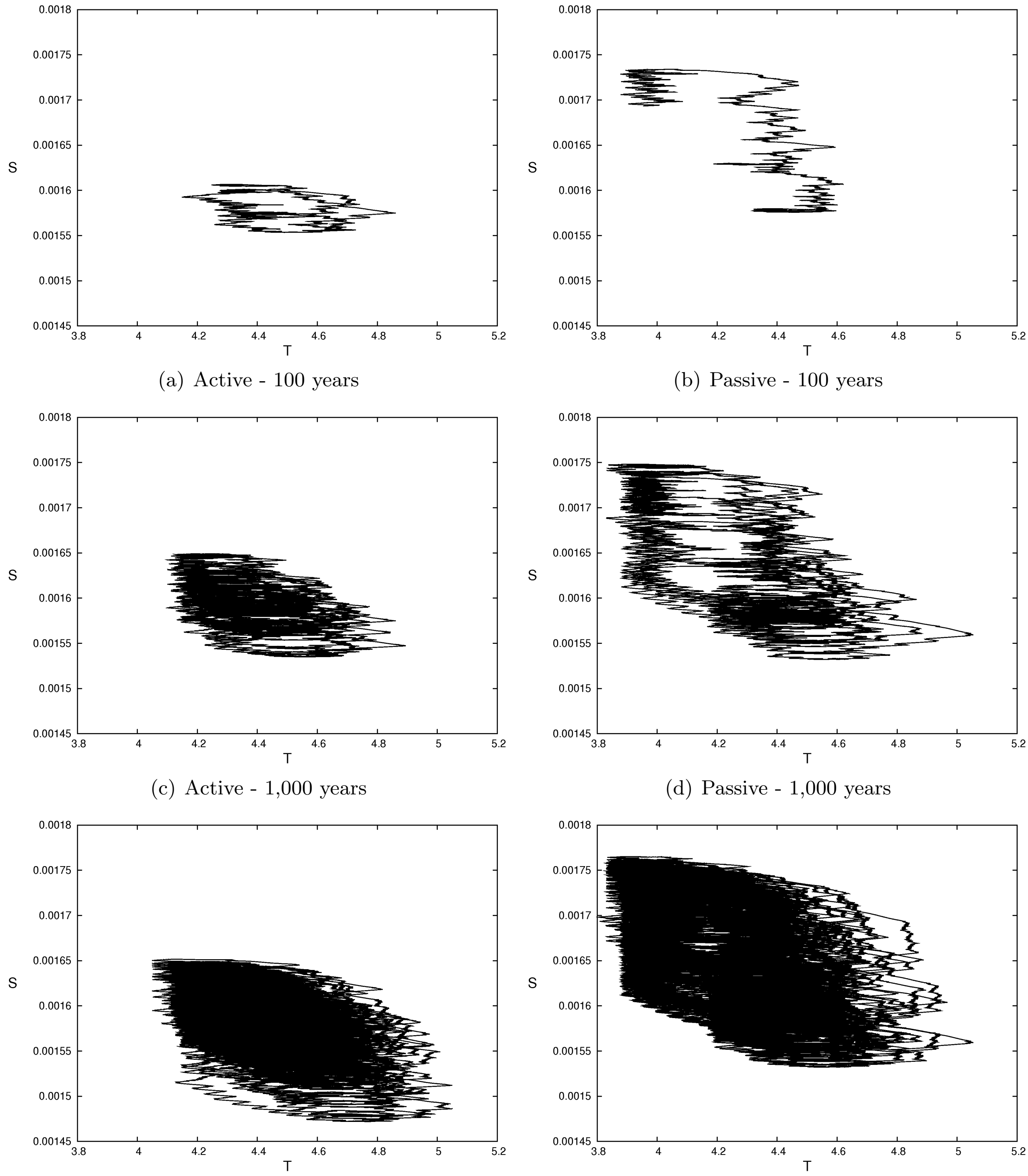

(a) Active - 100 years

(b) Passive - 100 years

(c) Active - 1,000 years

(d) Passive - 1,000 years

(e) Active - 10,000 years

(f) Passive - 10,000 years

Figure 5.2: Single trajectories of the ocean variables for simulations of the LS84 model over given time intervals. The plots in panels (a), (c) and (e) result from active coupling and (b), (d) and (f) result from passive coupling with associated ICs given in table 5.3.

is strongly influenced by the values of the coupling parameters. For passive coupling, shown in figure 5.3(b), in most (but not all) summers the trajectories move towards a model fixed point, before entering another phase of chaotic behaviour in the subsequent winter. However, in years two and six the trajectories display periodic behaviour in summer rather than moving towards a fixed point. For active coupling, the summer behaviour is more variable with four of the ten years displaying transitions towards a fixed point, two years displaying a mode of dense periodic behaviour and the remaining four years displaying an alternative mode of periodic behaviour. Lorenz (1990) comments on transitions between "active" and "inactive" summer circulation patterns in the L84 model stating that the resulting summer behaviour is dictated by the chaotic behaviour which occurs during the previous winter. It is therefore postulated that the recurrence of periodic and fixed-point summers in the seasonally driven LS84 model are determined by the chaotic transitions which occur in the preceding winter. On the evidence provided in figure 5.3 alone, the model atmospheric component's response to ocean coupling appears to be more variable under active coupling with at least three modes of summer behaviour evident.

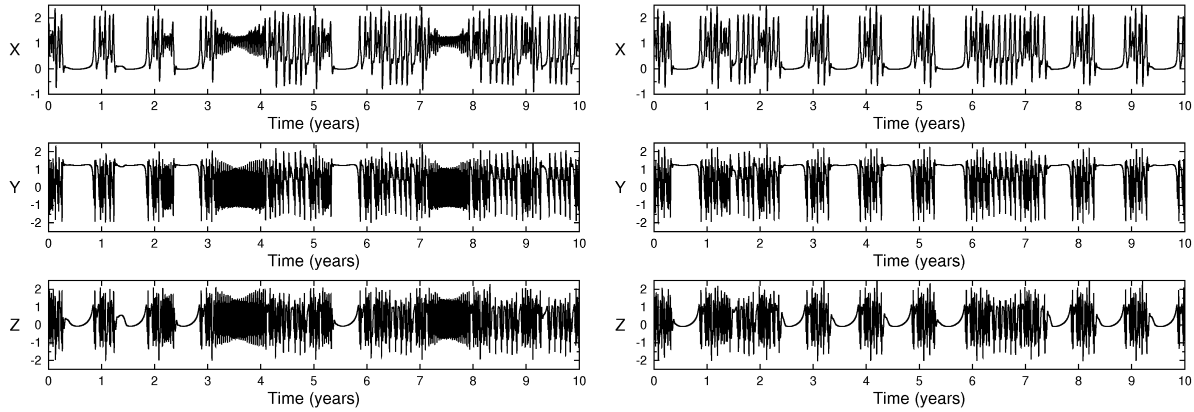

(a) Active (b) Passive

Figure 5.3: Atmospheric variables from single trajectory simulations of the LS84 model over a 10 year interval with (a) active coupling parameters and (b) passive coupling parameters using ICs given in table 5.3.

Figure 5.4 shows the evolution of the ocean variables T and S and the THC represented by f under active and passive coupling for the same model run depicted in figure 5.3 but for an extended period of 1,000 years. These figures reveal that various modes of variability are present in the ocean with considerable fluctuations occurring on decadal, multi-decadal and centennial time scales. As described in the previous section, in both coupling regimes, the inverse correlation between T and S is relatively clear with peaks in T broadly corresponding to troughs in S and vice versa. The time series shown in figure 5.4(b) displays two previously identified regimes centred at approximately $T = 4.0K$ and $T = 4.4K$ corresponding to high and low values of S respectively (consistent with figure 5.2(f)). The transitions between the high T, low S values (hereafter referred to as the HT regime) and the low T, high S values (hereafter referred to as the LT regime) occur at irregular intervals. Once a trajectory moves into one of these two regimes, the trajectory persists in the regime for many years before transitioning to the other regime. For example, at $t \approx 390$ years the trajectory spends approximately 100 years in the LT regime before transitioning to the HT regime for the following 80 years. The existence of regime behaviour suggests that under passive coupling, the model exhibits almost intransitive behaviour; assuming centennial time scales are considered 'long'. If the system was observed for relatively short time intervals (e.g. 100 years in this realisation), then it would be possible to observe only one of the two climate regimes; the implication being that a false interpretation of the model's climate would result. Furthermore, without an adequate understanding of the model's internal climate variability in the absence of trends in the model parameters, a transition to another regime may be misinterpreted as a change in climate. The transitions in T are more abrupt than the transitions in S suggesting a strong inertia in the response of the ocean salinity which is not as apparent in the ocean temperature.

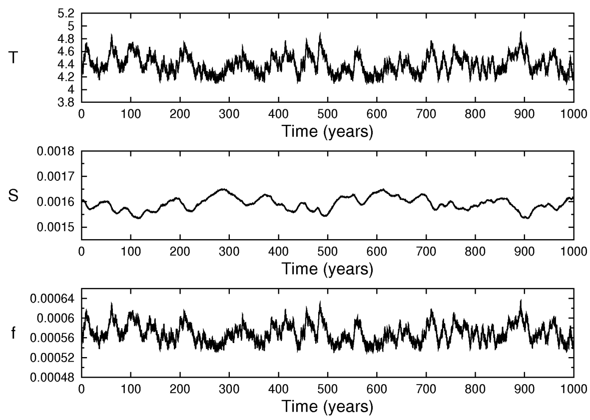

(a) Active

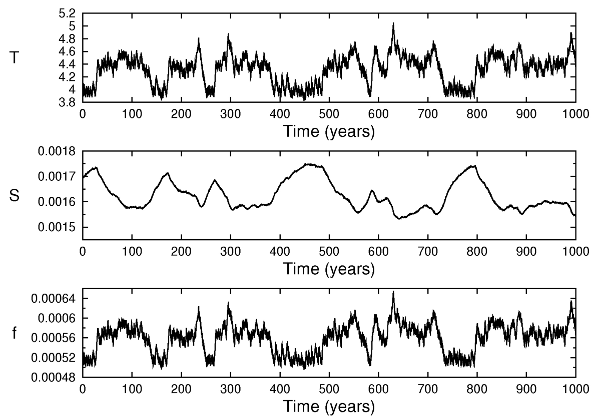

(b) Passive

Figure 5.4: Ocean variables from single trajectory simulations of the LS84 model over a 1,000 year interval with (a) active coupling parameters and (b) passive coupling parameters using ICs given in table 5.3.

When the model is subject to active coupling parameters, as shown in figure 5.4(a), there is considerable variability in the ocean on decadal and multi-decadal time scales but the time series does not reveal distinct regime behaviour on a centennial time scale. Abrupt changes in T are still observed and the time series in S similarly displays relatively slow changes in ocean salinity circulation. The trajectories propagate in different regions of state space under each mode of coupling, as shown by the different spread in the values of T and S.

For the parameter values and constants used in the experiments presented in this thesis, the ocean circulation (THC) is strongly driven by the ocean temperature difference, T. Therefore, changes in T dominate the response in f and this can clearly be seen in figure 5.4 as the time series for f closely resembles the time series in T. As the focus of this study is not on the behaviour of the THC per-se, subsequent plots of the ocean variables will be limited to T and S.

In order to further explore the differences between the two modes of coupling and provide a basis for running experiments to draw analogies to the climate system, the climate distributions of the model are determined using both the single trajectory model runs illustrated in figures 5.3 and 5.4, and by running large IC ensemble model simulations. The results are presented in section 5.3.

5.2.4 Almost intransitivity for passive coupling

In the analogy to the real climate system, one can consider the existence of regime behaviour in relation to the many modes of natural internal variability that are described in section 5.1. In the seasonally driven LS84 model, under passive coupling parameters, a long-term (multi-decadal to centennial) mode of internal variability is evident in the ocean variables from a single trajectory. Figure 5.4(b) shows the presence of two regimes which are most clearly seen in the T variable, referred to as the LT and HT regimes. Under active coupling parameters, variability exists on a number of time scales, as evidenced by the time series shown in figure 5.4(a), but it is more difficult to identify specific regions of the model state space which possess regime characteristics.

The occurrence of long-term internal variability relates to the transitivity of the model. Recall from section 2.1.4 that a transitive system is one in which a trajectory can pass through all of the possible system states and an intransitive system is one in which a trajectory will only pass through a subset of all possible system states; the subset is determined by the initial state and once established, will persist forever. According to Lorenz (1968):

> "In an almost intransitive system, statistics taken over infinitely long time intervals are independent of initial conditions, but statistics taken over very long but finite intervals depend very much upon initial conditions."

The definition of "very long" should be considered in relation to the system being studied. In the context of anthropogenic climate change, *very long* may therefore refer to behaviour which persists for many years, decades or perhaps even centuries.

When subject to active coupling parameters, the LS84 model appears to exhibit behaviour which can be considered transitive on multi-decadal to centennial time scales. However, over such time scales, almost intransitivity is apparent in the ocean variables under passive coupling parameters. The almost intransitive behaviour of the ocean in the LS84 model under passive coupling is of particular interest in the analogy to the climate system. Lorenz (1970) and Lorenz (1990) note that the climate system consists of subsystems operating on different time scales and explore the hypothesis that as a result the climate may be subject to almost intransitive behaviour. This is primarily because regime behaviour has been observed in the climate system on a number of temporal and spatial scales (from long-term global changes in glacial-interglacial cycles to shorter-term regional modes of variability such as the AMO). In addition, the capacity of a relatively simple nonlinear system to display regime behaviour with occasional abrupt transitions provides a valuable platform to develop a conceptual understanding of the role of internal climate variability in climate change prediction.

5.2.5 Impact of the ocean on the atmosphere

In this thesis, the focus is on determining the relevant experiments to run in order to produce climate model output which is usable and useful for the insurance sector and the wider adaptation community. Decisions regarding climate change adaptation, particularly within the insurance sector (described further in chapter six), are primarily concerned with changing atmospheric conditions (such as wind storms and precipitation events) but as the climate is a complex coupled system, the changing dynamics of subsystems such as the ocean have the potential to dominate future changes in atmospheric circulation. Whilst the intuitive response to producing more reliable model forecasts for atmospheric phenomena might be to better represent the atmosphere in a particular model, over increasing time scales the contributions of more slowly evolving components of the climate system, which ultimately constrain and control the atmospheric circulation, are likely to become increasingly important to accurate prediction. By analysing the behaviour of the LS84 model, the aim is to understand how sensitive a model's climate distributions are to uncertainty in the initial state of the ocean as well as the uncertainty in the atmosphere.

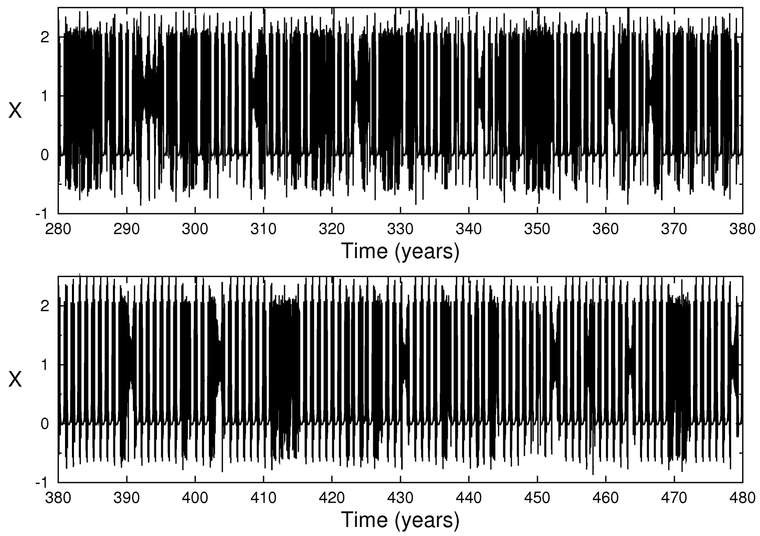

Figure 5.5: Time series of the X variable for a single LS84 model trajectory under passive coupling, initiated with ICs given in table 5.3. The top panel shows the time series for the interval between 280 and 380 years and the bottom panel shows the time series for the subsequent interval between 380 and 480 years.

To demonstrate the influence of the ocean on the atmospheric component of the LS84 model, figure 5.5 shows the evolution of the X variable over the interval from 280 to 480 years for the same model simulation used to generate figures 5.3(b) and 5.4(b). The top panel shows the trajectory from 280 to 380 years corresponding to the HT regime in figure 5.4(b) and the bottom panel shows the trajectory from 380 to 480 years which corresponds to the LT regime. When evolving in the LT regime, during the majority of summers (about 75%) the model trajectory evolves towards a model fixed point (at $X \approx 0.017$). However, in the HT regime the behaviour of X appears more erratic with only half of the summers showing the model moving towards the fixed point and the remainder exhibiting periodic oscillations. Figure 5.5 therefore serves to demonstrate that the state of the ocean has a discernible impact on the annual variability of the atmosphere. Appropriately accounting for uncertainty in the ocean state is therefore crucial in forecasting the evolution of the atmospheric variables. The following analysis is therefore focussed on predicting the behaviour of the ocean variables and investigating the implications of almost intransitivity for climate modelling.

5.3 The LS84 Model Climate Distributions

In this section, the climate of the seasonally driven LS84 model is determined for both active and passive coupling using single model trajectory distributions and IC ensembles distributions. The LS84 model has been shown to be chaotic when F_0 is fixed at $F_0 = 8$ and G_0 is fixed at $G_0 = 1$ (Van Veen et al. (2001)). If the model continues to exhibit chaotic behaviour and the model is shown to be transitive, then the single trajectory distributions will converge to the IC ensemble distributions over time demonstrating the ergodicity of the coupled model.

5.3.1 Single trajectory frequency distributions

Using the LS84 model runs for passive and active coupling described in section 5.2, with ICs listed in table 5.3, single trajectory frequency distributions are plotted for each model variable over increasing time periods. As in section 4.4.3, only one value per year is selected for each season (mid-winter/mid-summer) to ensure that the value of F_0 is identical at the instant each model state is extracted. Hence, a 100 year simulation includes 100 points.

Figures 5.6 and 5.7 show the frequency distributions for the S and T ocean variables respectively. The first column in each figure shows the distribution of states in mid-summer (when F_0 return to $F_0 = 6$) for active coupling; the second column shows the distribution of states in mid-winter (when F_0 return to $F_0 = 8$) for active coupling; the third column shows the distribution of states in mid-summer for passive coupling; and finally, the fourth column shows the distribution of states in mid-winter for passive coupling. Because the time scale of the ocean dynamics is approximately three orders of magnitude slower than that of the atmosphere in the LS84 model, the distributions for mid-winter and mid-summer are nearly identical for both active and passive coupling. Therefore, the plots shown in later sections of this chapter for the ocean variables are only given for mid-winter.

Under active coupling, figure 5.6 shows that the 100, 300 and 1,000 year distributions fail to span the entire range of possible values of S that are observed over longer simulation periods. Notably, after 1,000 years the trajectory has not visited the region in which $S < 1.53 \times 10^{-3}$, consistent with the plot shown for the T-S plane in figure 5.2(c). After 3,000 years, the trajectory has visited this region and the plots shown for 10,000 and 30,000 years do not vary considerably from the 3,000 year plot (see section 5.3.3 for a quantitative comparison) indicating that the distributions are converging. The converged distribution is a negatively skewed unimodal distribution with a peak at $S \approx 1.59 \times 10^{-3}$.

When the model is subject to passive coupling, the range of possible values of S is explored after 1,000 years, as shown in panels (o) and (p) but the 100 and 300 year distributions do not incorporate the region in which $S < 1.57 \times 10^{-3}$. The distribution after 3,000 years suggests a bimodal shape but the 10,000 and 30,000 year plots have more density in the higher of the two modal regions. Therefore, the distributions cannot be said to have converged until a period greater than 3,000 years. The converged distribution is bimodal with the lower modal region centred on $S \approx 1.59 \times 10^{-3}$ (as observed for active coupling) and the higher modal region revealing a peak at $S \approx 1.74 \times 10^{-3}$. In general, passive coupling leads to approximately half of the distribution density occurring where $S > 1.65 \times 10^{-3}$, associated with the LT regime and half occurring where $S < 1.65 \times 10^{-3}$, associated with the HT regime. The distributions for active coupling are limited to density only in the region in which $S < 1.65 \times 10^{-3}$. Therefore, under active coupling the equilibrium model behaviour is constrained to the HT regime, at least according to analysis based on the S variable.

The results plotted in figure 5.7 show the equivalent distributions for the T variable. Again, the mid-summer and mid-winter results are very similar but there are some differences in the exact location of the distribution peaks. The T distributions are also different under active and passive coupling. When the model is subject to active coupling, the behaviour is limited to the HT regime as all observed states occur at $T > 4.1K$. The general shape of the distribution is well approximated by the century-long simulations but the states in the tails of the distributions are only observed for longer simulation periods of at least 3,000 years.

Under passive coupling, figure 5.7 shows the bimodal nature of the distributions apparent in figure 5.6. The largely converged distributions for active coupling appear very similar to the upper model region of the T distributions (the HT regime) under passive coupling. In the 100, 300, 1,000 year plots (in panels *c*, *d*, *g*, *h*, *k* and *l*) and to a lesser extent in the 3,000 year plots (panels *o* and *p*), there is a disproportionately large area of density in the HT regime when compared to the distributions associated with longer periods. This shows that memory of the initial model sate is apparent in the single trajectory distributions for thousands of years. The implication is that a multi-thousand year single model simulation is required to approach the climate distributions for the ocean variables in the LS84 model. Without analysing the IC ensemble distributions, it is not possible to determine whether the eventual converged distributions associated with a single trajectory do in fact represent the full set of states consistent with the model parameters.

As discussed in section 5.2.5, the focus of the analysis presented in this chapter is on the predictability of the ocean variables because the evolution of the ocean controls the behaviour of the atmosphere and is of greater interest in the analogy to climate change. The frequency distributions for the atmospheric variables are shown in Appendix C, figures C-1 to **??**. The distributions show considerable differences between mid-winter and mid-summer because of the impact of the value of F $(F_0 + F_1T)$ on the model's underlying attractor. These differences are greater than those which arise because of the different coupling regimes.

5.3.2 IC ensemble distributions

A 10,000 member ensemble was initiated with ICs spread evenly along a transect spanning the range from $(X_1, Y_1, Z_1, T_1, S_1) = (-1.0, -2.5, -2.5, 3.8, 1.45 \times 10^{-3})$ to

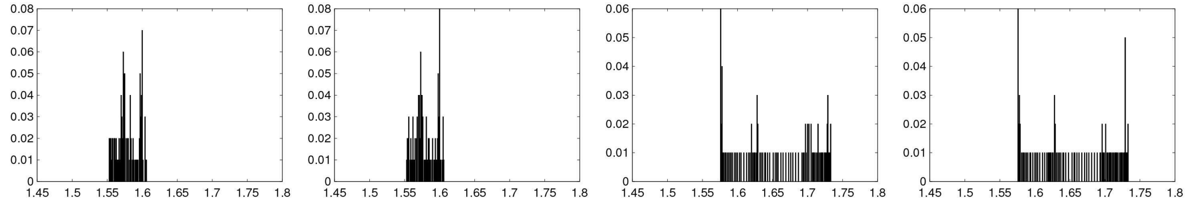

(a) 100 yrs, Active, Su (b) 100 yrs, Active, W (c) 100 yrs, Passive, Su (d) 100 yrs, Passive, W

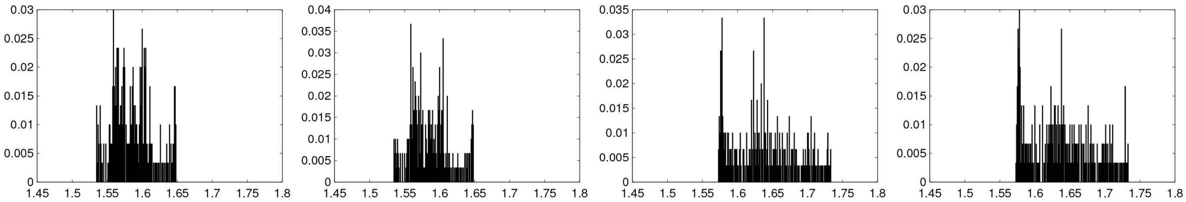

(e) 300 yrs, Active, Su (f) 300 yrs, Active, W (g) 300 yrs, Passive, Su (h) 300 yrs, Passive, W

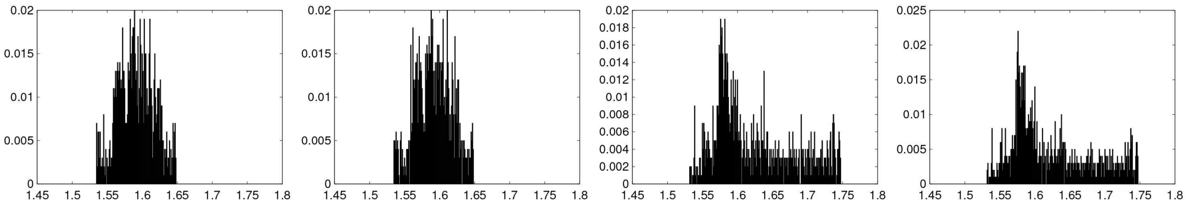

(i) 1,000 yrs, Active, Su (j) 1,000 yrs, Active, W (k) 1,000 yrs, Passive, Su (l) 1,000 yrs, Passive, W

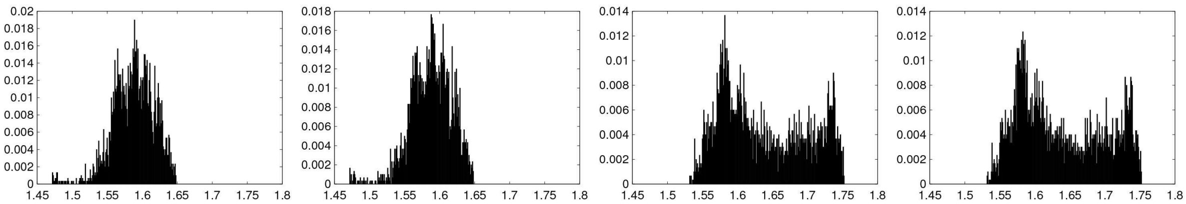

(m) 3,000 yrs, Active, Su (n) 3,000 yrs, Active, W (o) 3,000 yrs, Passive, Su (p) 3,000 yrs, Passive, W

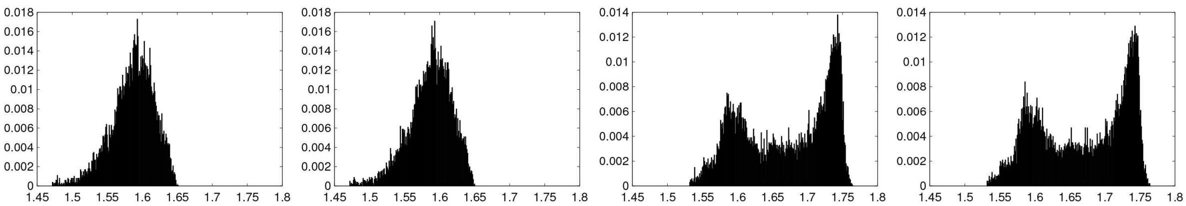

(q) 10,000 yrs, Active, Su (r) 10,000 yrs, Active, W (s) 10,000 yrs, Passive, Su (t) 10,000 yrs, Passive, W

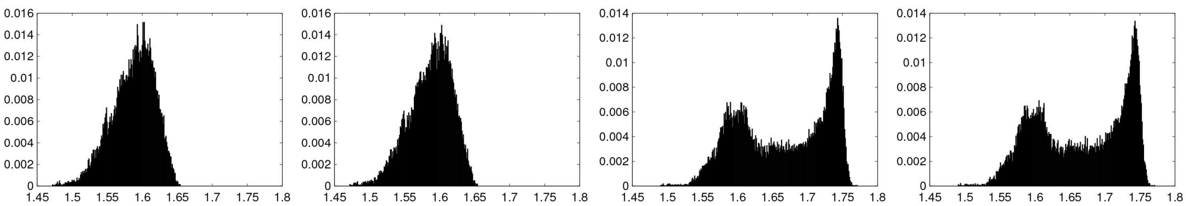

(u) 30,000 yrs, Active, Su (v) 30,000 yrs, Active, W (w) 30,000 yrs, Passive, Su (x) 30,000 yrs, Passive, W

Figure 5.6: Normalised frequency distributions for a single trajectory of the LS84 model variable S over increasing time periods. The method of coupling is given as active or passive and the respective ICs are given in table 5.7. *Su* denotes mid-summer and *W* denotes mid-winter. In each plot, the x-axis corresponds to ocean variable S ($\times 10^{-3}$) (psu) and the y-axis corresponds to the frequency per occupied bin; bin width $= 1 \times 10^{-6}$.

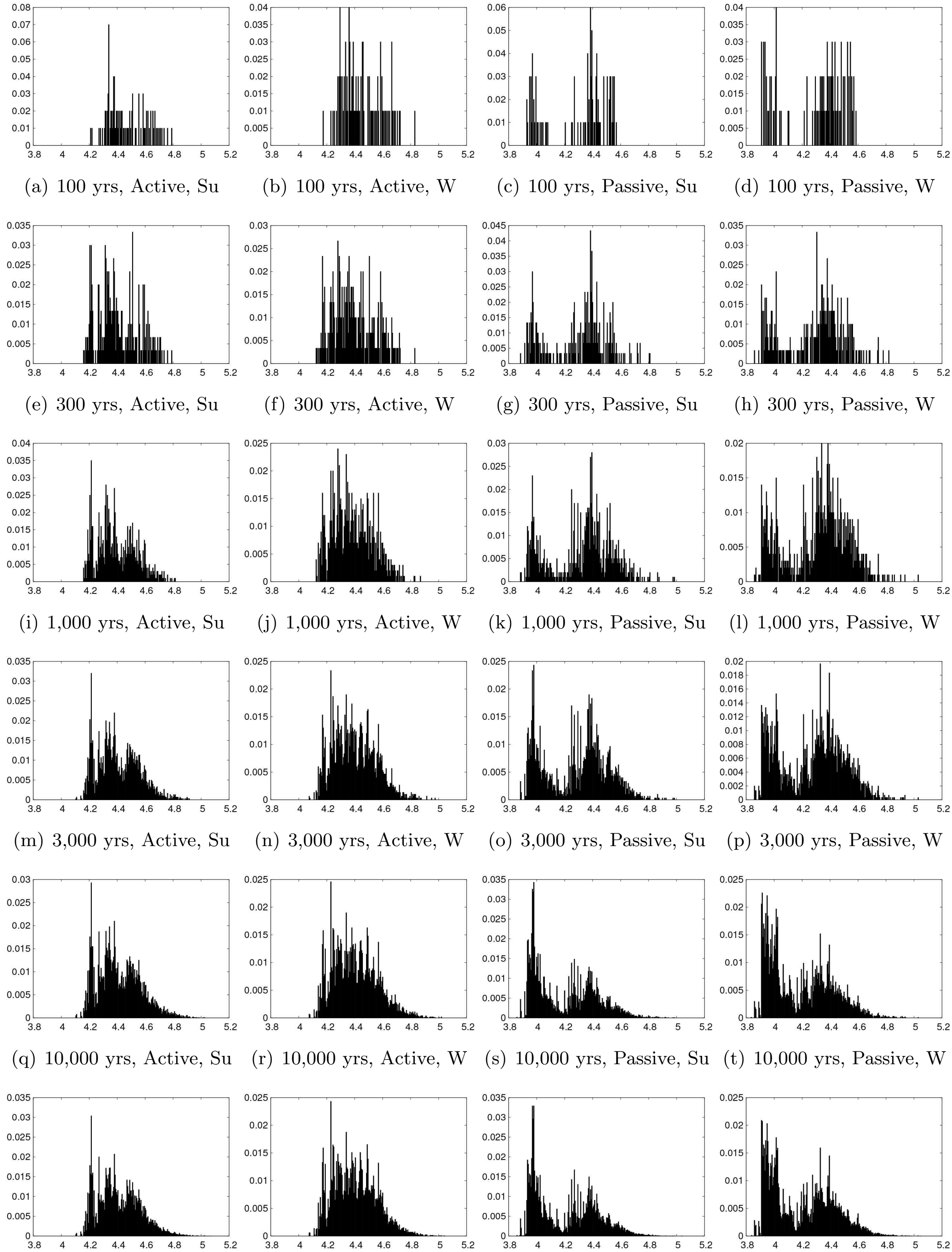

(a) 100 yrs, Active, Su (b) 100 yrs, Active, W (c) 100 yrs, Passive, Su (d) 100 yrs, Passive, W

(e) 300 yrs, Active, Su (f) 300 yrs, Active, W (g) 300 yrs, Passive, Su (h) 300 yrs, Passive, W

(i) 1,000 yrs, Active, Su (j) 1,000 yrs, Active, W (k) 1,000 yrs, Passive, Su (l) 1,000 yrs, Passive, W

(m) 3,000 yrs, Active, Su (n) 3,000 yrs, Active, W (o) 3,000 yrs, Passive, Su (p) 3,000 yrs, Passive, W

(q) 10,000 yrs, Active, Su (r) 10,000 yrs, Active, W (s) 10,000 yrs, Passive, Su (t) 10,000 yrs, Passive, W

(u) 30,000 yrs, Active, Su (v) 30,000 yrs, Active, W (w) 30,000 yrs, Passive, Su (x) 30,000 yrs, Passive, W

Figure 5.7: Normalised frequency distributions for a single trajectory of the LS84 model variable T over increasing time periods. The method of coupling is given as active or passive and the respective ICs are given in table 5.7. *Su* denotes mid-summer and *W* denotes mid-winter. In each plot, the x-axis corresponds to the ocean variable T (K) and the y-axis corresponds to the frequency per occupied bin; bin width $= 0.005$.

$(X_{10000}, Y_{10000}, Z_{10000}, T_{10000}, S_{10000}) = (2.5, 2.5, 2.5, 5.0, 1.8 \times 10^{-3})$. A transect between these values was selected assuming a knowledge of the range of model values but no information about the shape of the distributions. The ensemble is run for a period of 10,000 years. Figures 5.8 and 5.9 show the evolution of the ensemble at mid-winter at given time instants for the S and T variables respectively, under both active and passive coupling. Only mid-winter distributions are shown because the mid-summer distributions are very similar (as illustrated in section 5.3.1) due to the relatively slow evolution of the ocean variables. As previously stated, the long-term variability in the atmospheric variables (X, Y and Z) of the LS84 model is largely dominated by the dynamic behaviour of the ocean so analysis of the ocean variable distributions is most beneficial in extending the analogy to the climate system. The ensemble distributions for the atmospheric model variables are given in Appendix C, figures C-2 to C-4.

After three years of the model simulation with active coupling (see fig. 5.8(a)), the ensemble members remain fairly uniformly spread across the PA state space in the S dimension. After 30 years, the ensemble begins to converge to a smooth unimodal, negatively skewed distribution centred on $S = 1.6 \times 10^{-3}$. The general shape of the distribution remains unchanged for much longer simulation periods up to 10,000 years. The corresponding plots in T are less smooth, particularly at the lower range of the distribution, yet display a similar unimodal character centred on $T = 4.4$ with a positive skew.

When subject to passive coupling, the ensemble distributions appear to converge more slowly in the S variable. After 30 years (see fig. 5.8(k)), a bimodal distribution becomes apparent but the location of the upper modal region is lower than that observed after longer simulation periods. The converged distribution is bimodal with a primary peak at $S \approx 1.74 \times 10^{-3}$ and a secondary peak at $S \approx 1.59 \times 10^{-3}$ consistent with the converged single trajectory distribution after 10,000 years. The converged ensemble distributions for T also suggest a bimodal distribution consistent with converged single trajectory distributions but the convergence does not appear to be as slow as that observed in the S variable. The results support the observation made previously that a greater inertia is present in the ocean salinity as it responds slowly to changes in T.

The converged ensemble distributions are visually very similar to the distributions associated with long multi-thousand year single trajectory simulations. In the following section, the KS test is used to to investigate the ergodicity of the coupled model and provide quantitative estimates of the rates at which single trajectory frequency distributions converge to the reference climate distributions. In section 5.5, different IC ensembles from across the PA state space are run to explore how IC ensemble location affects the memory of the LS84 model.

5.3.3 Ergodicity in the LS84 model

In experiments with the L63 and L84 models, the ergodic assumption is shown to be valid when the parameters are fixed at values which lead to transitive behaviour. The versions of the LS84 model explored here are ultimately transitive but, as described in the previous section, when

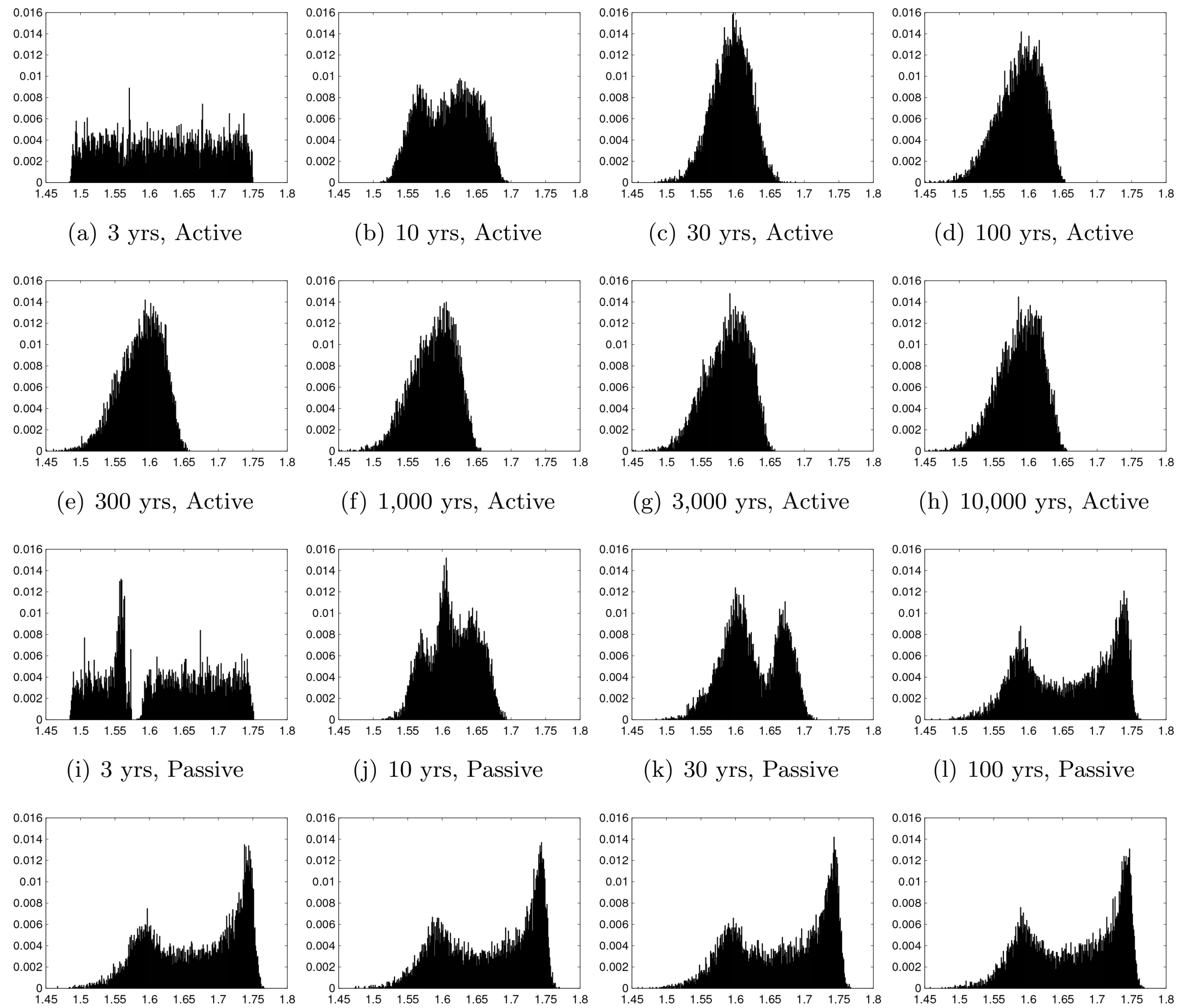

(a) 3 yrs, Active (b) 10 yrs, Active (c) 30 yrs, Active (d) 100 yrs, Active

(e) 300 yrs, Active (f) 1,000 yrs, Active (g) 3,000 yrs, Active (h) 10,000 yrs, Active

(i) 3 yrs, Passive (j) 10 yrs, Passive (k) 30 yrs, Passive (l) 100 yrs, Passive

(m) 300 yrs, Passive (n) 1,000 yrs, Passive (o) 3,000 yrs, Passive (p) 10,000 yrs, Passive

Figure 5.8: Normalised frequency distributions for the ocean variable S from a 10,000 member IC ensemble of the LS84 model in mid-winter at given instants in time. The method of coupling is given as active or passive and ICs are spread evenly along a transect spanning the range from $(X_1, Y_1, Z_1, T_1, S_1) = (-1.0, -2.5, -2.5, 3.8, 1.45 \times 10^{-3})$ to $(X_{10000}, Y_{10000}, Z_{10000}, T_{10000}, S_{10000}) = (2.5, 2.5, 2.5, 5.0, 1.8 \times 10^{-3})$. In each plots the x-axis corresponds to S ($psu \times 10^{-3}$) and the y-axis corresponds to the frequency of ensemble members per occupied bin; bin width $= 1 \times 10^{-6}$.

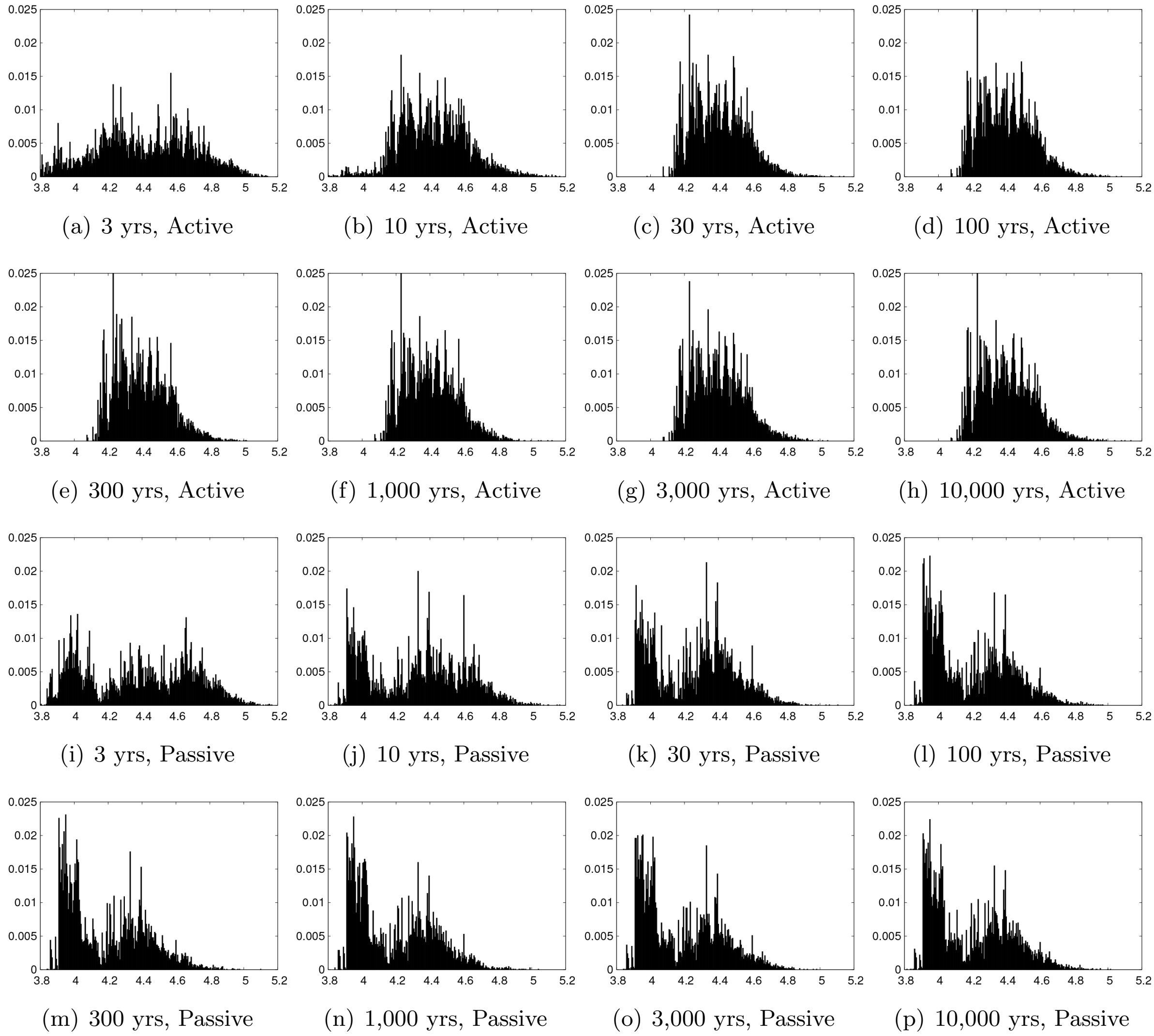

(a) 3 yrs, Active (b) 10 yrs, Active (c) 30 yrs, Active (d) 100 yrs, Active

(e) 300 yrs, Active (f) 1,000 yrs, Active (g) 3,000 yrs, Active (h) 10,000 yrs, Active

(i) 3 yrs, Passive (j) 10 yrs, Passive (k) 30 yrs, Passive (l) 100 yrs, Passive

(m) 300 yrs, Passive (n) 1,000 yrs, Passive (o) 3,000 yrs, Passive (p) 10,000 yrs, Passive

Figure 5.9: Normalised frequency distributions for the ocean variable T from a 10,000 member IC ensemble of the LS84 model in mid-winter at given instants in time. The method of coupling is given as active or passive and ICs are spread evenly along a transect spanning the range from $(X_1, Y_1, Z_1, T_1, S_1) = (-1.0, -2.5, -2.5, 3.8, 1.45 \times 10^{-3})$ to $(X_{10000}, Y_{10000}, Z_{10000}, T_{10000}, S_{10000}) = (2.5, 2.5, 2.5, 5.0, 1.8 \times 10^{-3})$. In each plot, the x-axis corresponds to T (K) and the y-axis corresponds to the frequency of ensemble members per occupied bin; bin width = 0.005.

the model is passively coupled trajectories display almost intransitive behaviour. The length of time over which the model must be run to ensure that a single model realisation produces 'climate' statistics representative of the underlying PA is investigated for both passive and active coupling parameters. The analysis in this section again focusses on the ocean variables.

The 10,000 member IC ensemble and single trajectory distributions are compared to reference "climate" distributions shown in figure 5.10. These ensemble distributions consist of 100,000 members, with ICs spread evenly along a transect spanning the range from $(X_1, Y_1, Z_1, T_1, S_1) = (-1.0, -2.5, -2.5, 3.8, 1.45 \times 10^{-3})$ to $(X_{100000}, Y_{100000}, Z_{100000}, T_{100000}, S_{100000}) = (2.5, 2.5, 2.5, 5.0, 1.8 \times 10^{-3})$, after a simulation period of 1,000 years. Running a 100,000 member ensemble generates more precise estimates of the model climate distributions than a 10,000 member ensemble. A period of 1,000 years is chosen based on the ensemble results in section 5.3.2 which suggest that memory of the original IC ensemble location is lost on the order of hundreds of years.

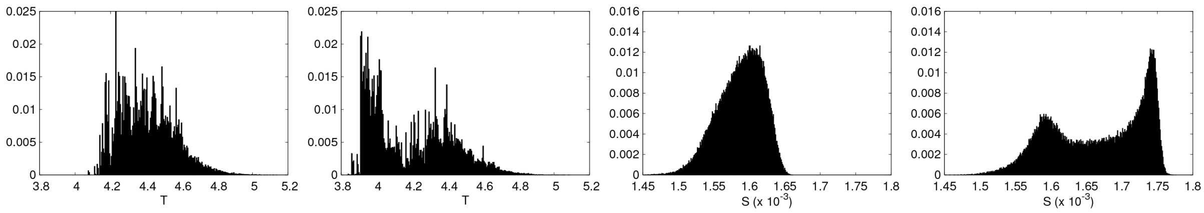

(a) T, Active (b) T, Passive (c) S, Active (d) S, Passive

Figure 5.10: Normalised frequency distributions for the ocean variables after a 1,000 year simulation from a 100,000 member IC ensemble of the LS84 model in mid-winter. The method of coupling is given as active or passive and ICs are spread evenly along a transect spanning the range from $(X_1, Y_1, Z_1, T_1, S_1) = (-1.0, -2.5, -2.5, 3.8, 1.45 \times 10^{-3})$ to $(X_{10000}, Y_{10000}, Z_{10000}, T_{10000}, S_{10000}) = (2.5, 2.5, 2.5, 5.0, 1.8 \times 10^{-3})$. In each plot, the y-axis corresponds to the frequency of ensemble members per occupied bin; bin width = 0.005 for T and 1×10^{-6} for S.

The frequency distributions associated with single trajectory simulations of increasing periods, some of which are illustrated in figures 5.6 and 5.7, are compared to the IC ensemble distributions shown in figure 5.10 which represent the model climate distributions under each coupling regime. The KS test is used to compare the distributions and the results are shown in figure 5.11.

The plots in figure 5.11 show the KS comparisons for the T and S variables over the 100,000 year time period for both active and passive coupling parameters. In both coupling regimes the single trajectory distributions eventually converge towards the ensemble climate distributions, indicated by the decrease in D over time towards $D = 0$. The ergodic assumption is therefore valid provided the model is run for a *sufficiently* long simulation period. In the LS84 model versions explored here, a *sufficient* simulation period is dependent on the values of the coupling parameters.

The results show that convergence is slower under passive coupling (fig. 5.11(b)) because of

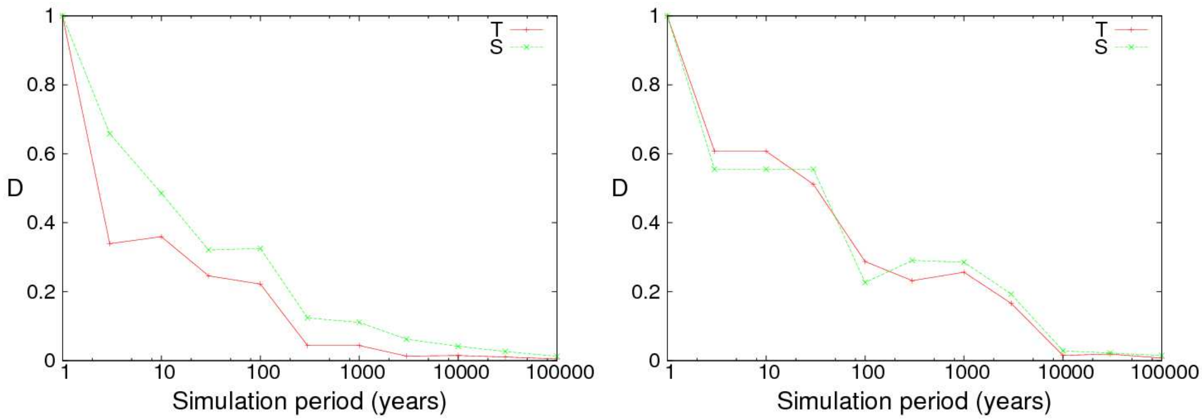

(a) Active (b) Passive

Figure 5.11: KS comparisons between single model trajectories of increasing simulation periods (using ICs given in table 5.3) and the 100,000 member IC ensemble "climate" distributions (shown in figure 5.10) for both active and passive coupling parameters.

the long-term internal variability between the HT and LT regimes causing the model to display almost intransitive behaviour. A 10,000 year single trajectory simulation is required before D approaches $D = 0$ for both ocean variables. Under active coupling (fig. 5.11(a)), the convergence is more rapid but a simulation period of hundreds and perhaps even thousands of years is still required before the ergodic assumption can be considered valid. Also, because of the slow response of the salinity component of the ocean model, the convergence is slower in the S variable than in the T variable. This result is clear under active coupling but the convergence appears to occur at a similar rate for both T and S under passive coupling. However, as the simulation period increases, the inertia in S is once again evident. The appropriate use of the ergodic assumption therefore appears to be not only time scale dependent but also variable dependent.

As the duration of the sample from a single trajectory increases one would expect the 'climate' statistics of the trajectory to converge towards those of the ensemble climate distributions. Whilst this is broadly what is observed, the trends in D are not smooth. As evident in figure 5.11(b), increasing the simulation period from 100 to 3,000 years does not lead to sizeable decreases in the magnitude of D in either of the ocean variables. In the S variable, the value of D actually increases after a 1,000 year simulation compared to a 100 year simulation which suggests that increasing the simulation length, for a system which displays almost intransitivity, will not necessarily render the ergodic assumption valid. The internal variability in the system means that a single trajectory may spend a disproportionate period of time in a particular regime of the PA causing the frequency distributions to diverge from the ensemble climate distributions.

If the climate system is almost intransitive on spatial scales and temporal scales relevant to climate change adaptation, then using a single simulation to estimate the PDF of a particular climate variable to estimate exceedance probabilities will be misleading. The results shown using the LS84 model suggest that even if there are no trends in the forcings, increasing the simulation period doesn't always improve the viability of the ergodic assumption. Large IC ensembles are therefore required to estimate the climate distributions of the model. The obvious question that follows is how big IC ensembles need to be in order to provide reliable quantitative estimates of climate variable distributions. This question has so far been side-stepped in this thesis but the next section provides some guidance using the LS84 model.

5.4 Using IC Ensembles to Inform Probabilities

5.4.1 IC ensemble size

Throughout the thesis it is argued that in the analogy to climate, the model results support the case for running large IC ensembles to establish the range of behaviour consistent with the climate system's forcings. However, the issue of an appropriate ensemble size has not been addressed. This is largely due to the abstract relationship between the experiments conducted on the L63, L84 and LS84 models and experiments performed using complex GCMs but also because the primary focus has been on establishing the need (if any) for IC ensembles in climate change prediction rather than in optimising the design of IC ensemble experiments. Furthermore, the link between IC ensemble based forecasts and probabilistic information of climate and climate change has not been discussed thus far in the results. Experiments analysing the L63 and L84 model behaviour were directed towards developing a conceptual understanding of climate under altered forcing conditions and therefore focussed primarily on the concepts of transitivity, ergodicity and IC memory. Here, the LS84 model allows analysis of a system with two different time scales and the distinct regime behaviour in the ocean variables under passive coupling presents an opportunity to investigate the impact of IC uncertainty (and IC ensemble size) on the probability of transitioning between defined regimes. Having developed a conceptual framework and the appropriate language for understanding climate in a nonlinear chaotic system in previous chapters, the analysis shown here attempts to provide further guidance for climate model experimental design in order address decisions which can be informed by characterisation of uncertainties in relation to probabilities. This section explores the issue of ensemble size using the LS84 model under passive coupling, in the absence of any trends in the forcing parameters. The aim is to determine the minimum IC ensemble size necessary to provide robust quantitative estimates of the probabilities associated with the climate distributions of the LS84 model.

5.4.2 Experimental design

Utilising the previously identified HT and LT regimes evident in the ocean variables under passive coupling, an experiment is performed to estimate the probability of a trajectory being in a particular regime as a function of lead time. Ensembles of increasing size are investigated to understand how many ensemble members are required to give a reliable assessment of the model PDFs after a given simulation period. The HT and LT regimes are therefore given explicit quantitative ranges. A trajectory is determined to be in either of the two regimes based on the value of T. If $T > 4.25$, the state is in the HT regime and if $T < 4.1$ the state is in the LT regime. If T is in the range $4.1 < T < 4.25$ then the state is considered to be *ambiguous*. For example, in the time series of T shown in figure 5.4(b), the model trajectory initially evolved in the LT regime for 20 years before transitioning to the HT regime.

The ICs of the ensemble members are determined by generating coordinates close to an initial state $(X_{IC}, Y_{IC}, Z_{IC}, T_{IC}, S_{IC}) = (1.087, 1.129, 0.635, 3.949, 1.693 \times 10^{-3})$. For an ensemble of size N (in this example $N = 10,000$) each ensemble member, i for $i = 1, 2, ..., N$, is assigned an initial state according to the coordinates:

$$(X_i, Y_i, Z_i, T_i, S_i) = (X_{IC} + r_{xi}, Y_{IC} + r_{yi}, Z_{IC} + r_{zi}, T_{IC} + r_{Ti}, S_{IC} + r_{Si})$$

where r_{xi}, r_{yi} and r_{zi} are randomly generated numbers from a three-dimensional uniform distribution in a sphere with a radius, $rad = 0.1$, centred on $(0, 0, 0)$; and r_{Ti} and r_{Si} are random numbers from one-dimensional uniform distributions in the ranges $-0.02 < r_{Ti} < 0.02$ and $-2 \times 10^{-5} < r_{Si} < 2 \times 10^{-5}$ respectively.

Initially all ensemble members are in the LT regime. For a selection of lead times, the percentage of ensemble members in the LT regime and the percentage in the HT regime are calculated. Those trajectories which are in the region where $4.1 < T < 4.25$ are labelled ambiguous. 17 ensembles of increasing sizes are investigated, with the number of ensemble members (E) given by $E = 2^{n-1}$, where $n = 1, 2...17$. The minimum ensemble size is therefore 1 member and the maximum size is 65,536 members.

5.4.3 Ensemble size results

The percentage of ensemble members in each regime is plotted against E for lead times of 3, 10, 30 and 100 years. One would expect that the probability of a transition to the HT regime would increase with lead time. This is indeed what is observed in the results illustrated in figure 5.12. After three years the ensemble results display convergence to a result where approximately 81% of members are in the LT regime, 3% are now located in the HT regime and the other 16% are classed as ambiguous. When the lead time is extended to 100 years, the probability of the trajectory being in the HT regime increases to nearly 40% while the number of ensemble members in the LT regime decreases to less than 50%.

The results of the experiment show that the probability estimates converge as the ensemble size increases for each lead time investigated. Furthermore, increasing the ensemble size beyond a certain threshold does not lead to significant improvements in the estimates of the regime probabilities. In all of the plots shown in figure 5.12, an ensemble size of approximately 2,000 to 4,000 members appears sufficient to provide a reliable estimate of the percentage of trajectories in the LT regime, the HT regime and those which are ambiguous. When the LS84 model is subject to almost intransitive behaviour and there is no trend in the model parameters, an ensemble size of approximately 2,000 to 4,000 is therefore sufficient to estimate the broad statistical properties of the model climate distributions. However, in estimating the probabilities of more extreme events, such as the probability of a trajectory where $T > 5$, increasing the size of the ensemble further still is expected to generate more reliable probability estimates. Further experiments with the LS84 model could be performed to establish the necessary ensemble sizes to determine robust estimates of the probabilities of rare/tail events.

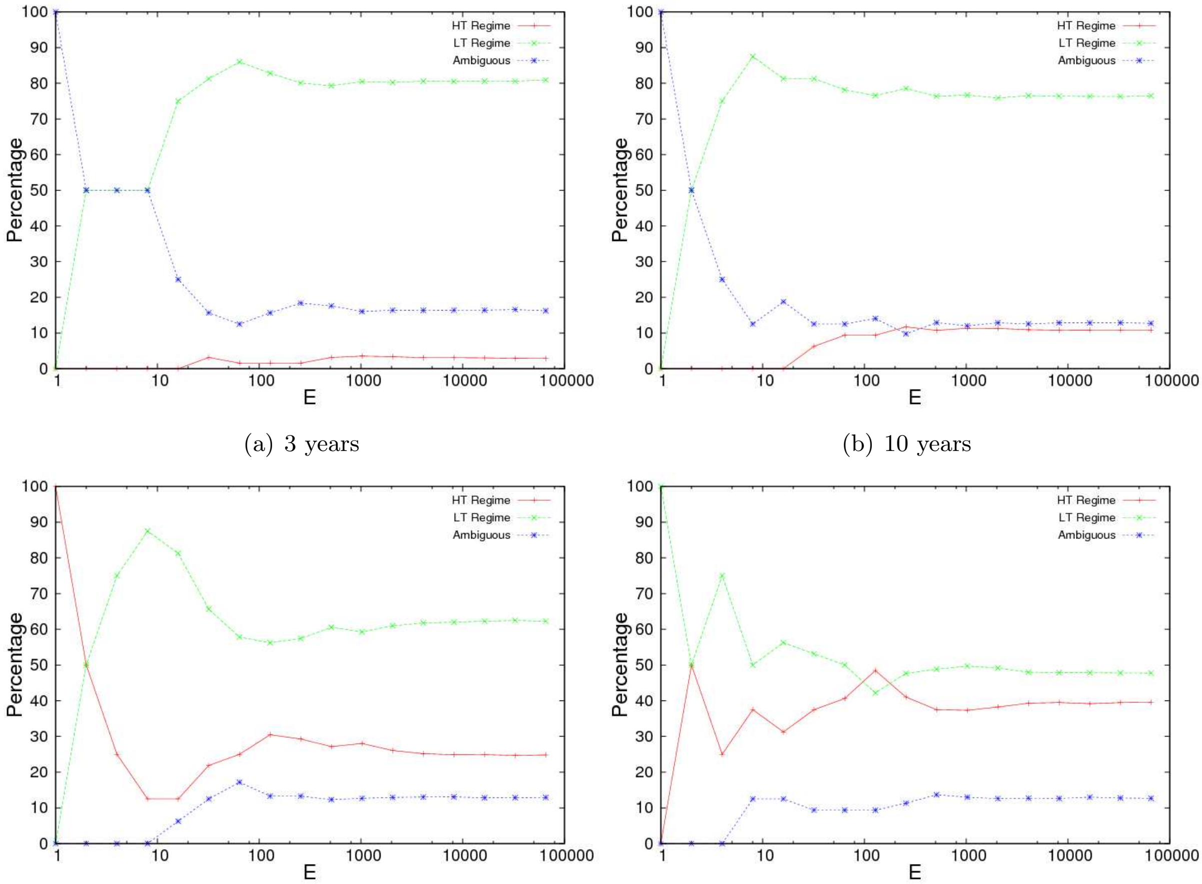

(a) 3 years

(b) 10 years

(c) 30 years

(d) 100 years

Figure 5.12: The percentage of ensemble members remaining in the LT ($T < 4.1$), having transitioned to the HT regime ($T > 4.25$) and those which are ambiguous ($4.1 < T < 4.25$) as a function of ensemble size for simulation periods of (a) 3 (b) 10 (c) 30 and (d) 100 years in the LS84 model under passive coupling. The ensembles members are initiated with ICs close to a reference state $(X_i, Y_i, Z_i, T_i, S_i) = (1.087, 1.129, 0.635, 3.949, 1.693 \times 10^{-3})$.

5.4.4 Convergence of prediction lead times

The experiment designed to explore ensemble size can be adapted to study the lead time at which memory of the IC ensemble location is lost. Previously, the probability of a trajectory being located in a particular regime is determined for increasing ensemble sizes. In this section, the experimental design is inverted so that rather than focussing on a specific lead time and varying the ensemble size, the ensemble size is fixed and the lead time is varied. Ensemble simulations are performed for increasing lead times (up to 1,000 years) using three ensemble sizes, where $E = 2^4$, 2^8 and 2^{12}. The aim is to establish the lead time at which the percentages stabilise, providing a measure of the memory of ICs in the model. Figure 5.13 shows the convergence in the percentage of members in the LT and HT regimes as a function of the model simulation lead time.

When $E = 2^4$ (see fig. 5.13(a)) the percentage of trajectories in each of the regimes changes

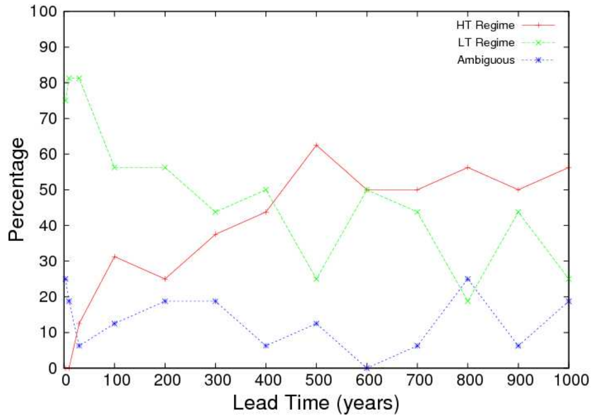

(a) $E = 2^4 = 16$

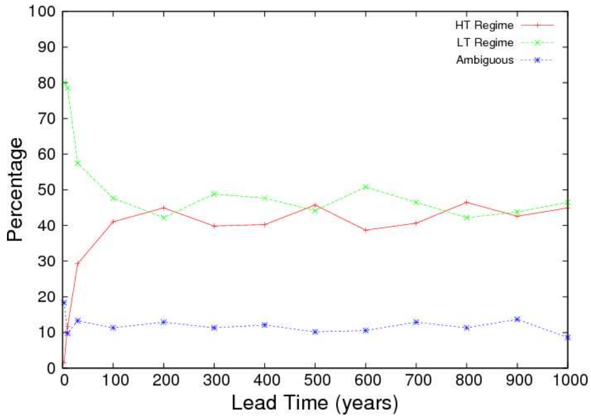

(b) $E = 2^8 = 256$

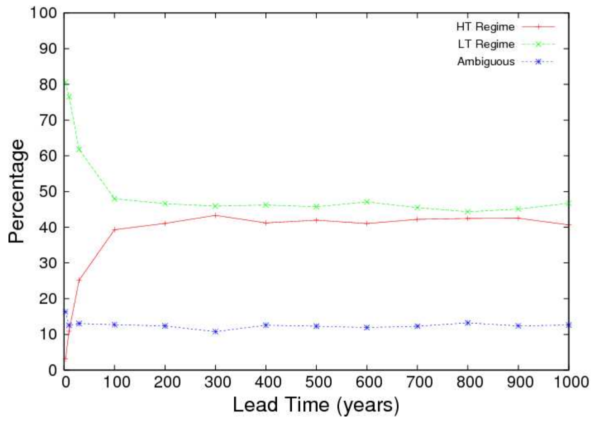

(c) $E = 2^{12} = 4096$

Figure 5.13: The proportion of ensemble members in the LT ($T < 4.1$), HT ($T > 4.25$) and ambiguous ($4.1 < T < 4.25$) regimes as a function of lead time for ensemble sizes of (a) 16 (b) 256 and (c) 4096 in the LS84 model under passive coupling. The ensembles members are initiated with ICs close to a reference state $(X_i, Y_i, Z_i, T_i, S_i) = (1.087, 1.129, 0.635, 3.949, 1.693 \times 10^{-3})$.

considerably at each time instant. As a consequence of a limited number of ensemble members, the experiment is relatively uninformative regarding the memory of ICs in the LS84 model. For a larger ensemble, when $E = 2^8$ (see fig. 5.13(b)), the experimental results are more informative. The percentage of trajectories in the LT regime decreases over the first 200 to 300 years of the model simulation. For lead times of 200 to 1,000 years, the percentage of trajectories in either the LT or HT regime oscillates between 40 to 50%. The result suggests that for at least 100 years and perhaps even 200 or 300 years, the PDFs of the LS84 model variables are a function of the IC ensemble location. In figure 5.13(c), when the ensemble size is increased to $E = 2^{12}$, convergence of the percentages occurs after 200 years. The percentages are also more constrained and for lead times of 200 to 1,000 years the percentage of ensemble members in the HT regime converges to approximately 42%, the percentage in the LT regime converges to approximately 46% and the remaining 12% are considered ambiguous.

In this section, the memory of ICs in the LS84 model has been investigated but the analysis has been limited to a single IC ensemble originating in the LT regime. In the next section, the sensitivity of the IC ensemble distributions to the initial location of the ensemble on the model's PA is investigated to determine whether or not the model memory is a function of IC location.

5.5 Memory in the LS84 Model

5.5.1 Experimental design

The time it takes for the distributions associated with two different IC ensembles to converge provides a measure of the memory in the LS84 model. For a system which has coexisting attractors and displays intransitivity, the ensembles will never fully converge (assuming the ensembles span more than one basin of attraction). If the system is transitive, the ensembles will eventually converge but if that time is long relative to the dynamic time scale of the system then the system can be considered almost intransitive. In this section, the rates of convergence between the distributions associated with four different IC ensembles are compared when the LS84 model is subject to passive coupling. As explained in section 5.2.4, analysing the model under passive coupling can provide useful insights into the predictability of the climate system which displays regime behaviour and therefore may also be subject to almost intransitive behaviour.

Variable	IC 1	IC 2	IC 3	IC 4
X	1.087	0.439	0.625	0.303
Y	1.129	0.470	1.084	0.790
Z	0.635	1.133	-0.844	0.979
T	3.949	3.993	4.343	4.300
S ($\times 10^{-3}$)	1.693	1.723	1.686	1.628

Table 5.4: ICs used as the centre of the four IC ensembles investigated in section 5.5.

The four IC ensembles are centred on observed states from the single trajectory plots shown in section 5.2. The ICs are given in table 5.4. The IC state referred to as *IC 1* is the initial state used for the single trajectory simulation under passive coupling. *IC 2* is the state observed after 20 years of that particular model run, *IC 3* is the state observed after 40 years of the model run and *IC 4* is the state observed after 60 years of the model run. These four IC states are chosen because the first two states are located in the LT regime and the second two are located in the HT regime. The aim is to establish and compare the rates at which IC ensembles converge when originating in the same regimes and in different regimes.

Using the four states listed in table 5.4 as the central coordinates of the IC ensembles, the 10,000 individual members for each ensemble are given slightly different ICs according to the coordinates given in section 5.4.2 where $(X_{IC}, Y_{IC}, Z_{IC}, T_{IC}, S_{IC})$ is the reference state from table 5.4 and the other variables are the same as those defined in section 5.4.2. The ICs for each ensemble are illustrated in figures 5.14(a) and 5.14(b) for the atmosphere and ocean variables respectively. The figures are reproductions of figure 5.1(b) and figure 5.2(b) with the locations of the IC ensembles superimposed.

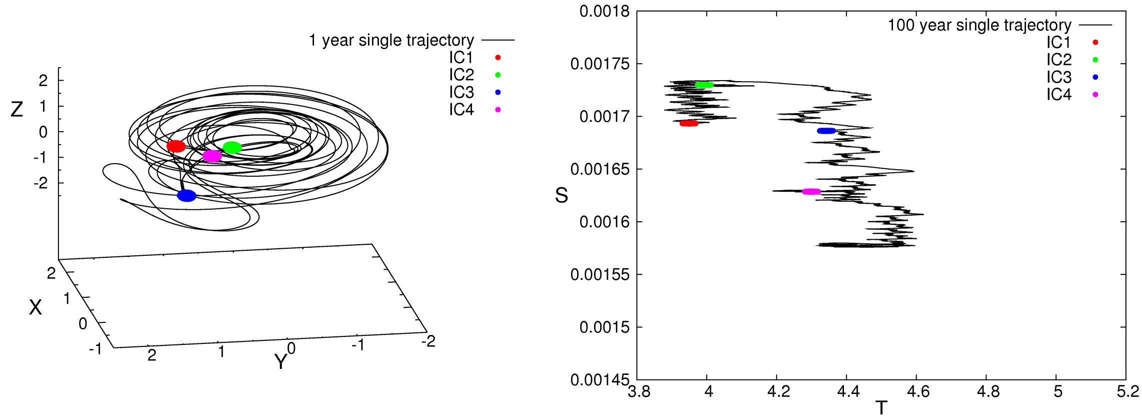

(a) Atmosphere (b) Ocean

Figure 5.14: Four 10,000 member IC ensembles superimposed on the model pseudo-attractor of the LS84 model under passive coupling parameters in: (a) the atmospheric variables, X, Y and Z; and (b) the ocean variables, T and S.

5.5.2 IC ensemble distributions

Plotting using a 3D colour-map

Throughout the thesis, frequency distributions have been presented in the form of two-dimensional histograms. The KS test has also been employed to provide statistical comparisons between distribution results over time. To reduce the number of plots shown in this section and subsequent sections, an alternative plot-type is used. A 3-dimensional colour-map is utilised to show how frequency distributions vary in time. The colour-map consists of two axes for the variable and time dimensions while the third dimension, the frequency within each variable bin, is expressed using a colour scale with a gradient between two colours (white and blue) where the darker the shade, the higher the frequency. In the 3D colour-map plots, the values given to the right of each figure correspond to the frequency of states per bin. The temporal resolution of the data dictates the width of each distribution plotted. In the following plots, data is extracted every ten years so the first ten years of the time series' in the 3D plots denotes the distribution at time $t = 0$ years (mid-winter), the next ten years denotes the distribution at $t = 10$ years (mid-winter) and so on.

IC ensemble results

The results presented in figures 5.15 and 5.16 show the evolution of the different IC ensembles over a 250 year period at 10 yearly intervals. Figures 5.15(a) and 5.15(b) show the response in the T variable of the IC ensembles originating in the LT regime and figures 5.15(c) and 5.15(d) show the response in the T variable of the IC ensembles originating in the HT regime. Over the first few decades of the model simulation, the ensemble members remain in their original

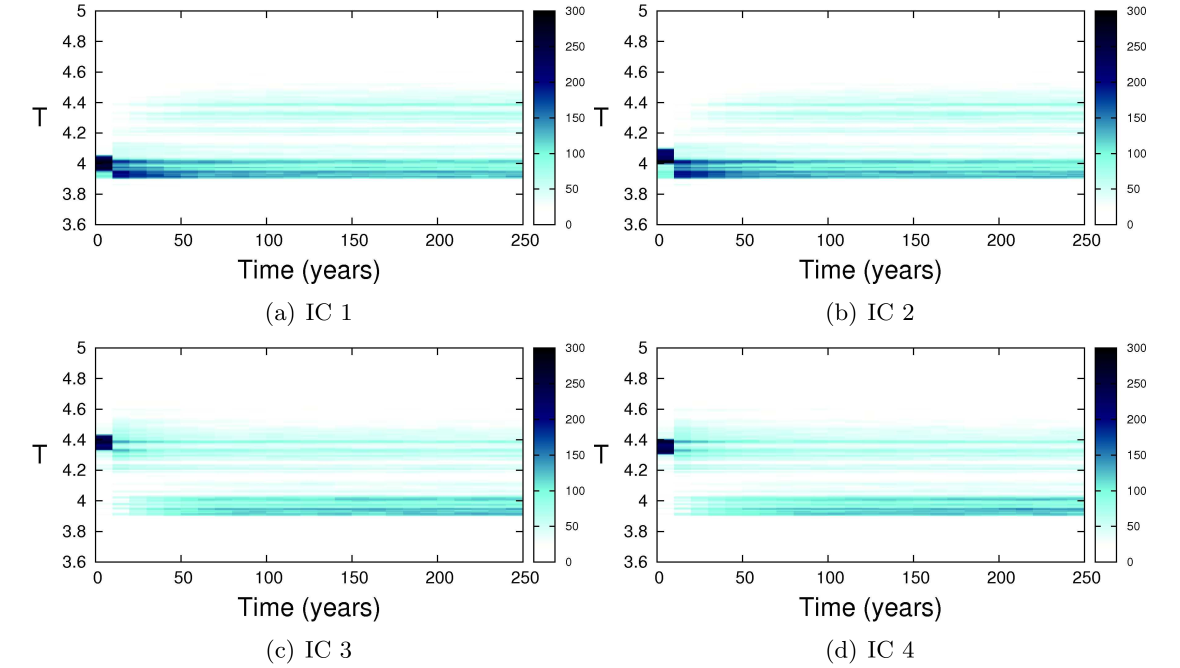

Figure 5.15: 3D colour-map showing the evolution of the four ensembles illustrated in figure 5.14 for the T variable.

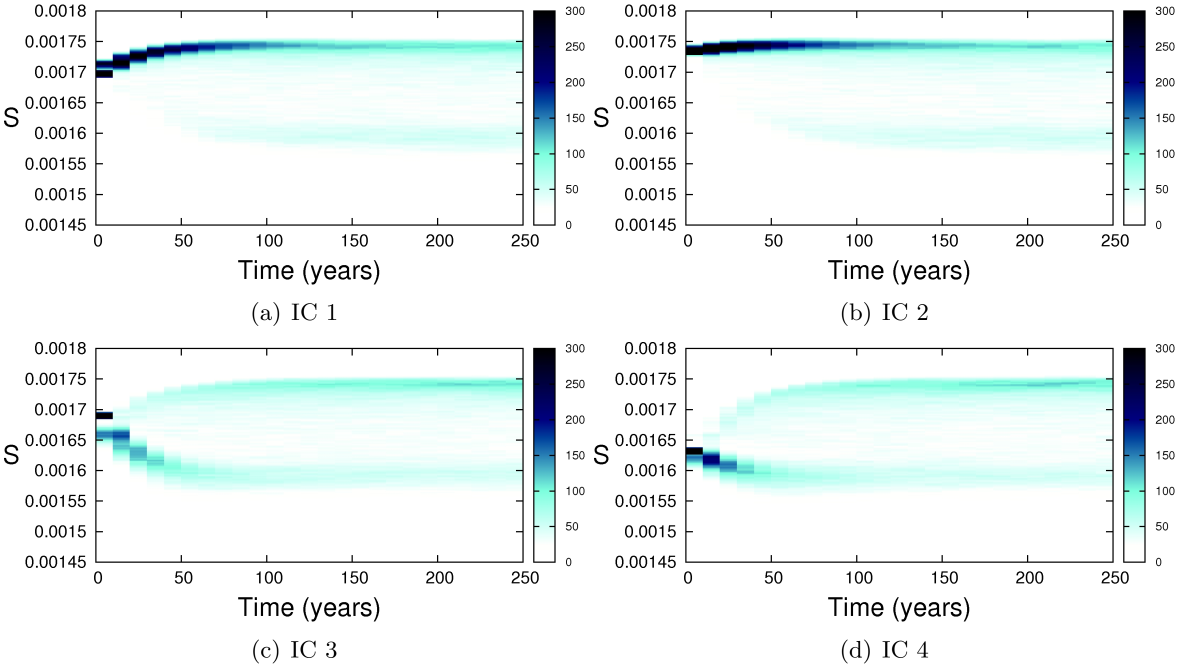

Figure 5.16: 3D colour-map showing the evolution of the four ensembles illustrated in figure 5.14 for the S variable.

regimes but over time the ensemble members spread across the PA state space and the ensemble distributions from both regimes appear to converge. The results for the S variable show that the ensembles from *IC 1* and *IC 2* evolve in a similar way with the majority of members moving initially towards high values of S. Conversely, the majority of ensemble members from the ensembles labelled *IC 3* and *IC 4* initially move towards low values of S. Although ensembles *IC 1* and *IC 3* initiate from regions of state space with very similar values in S, because the behaviour of the model is temperature driven (see section 5.2.3), the evolution of model trajectories is dominated by the initial values of T. Therefore, irrespective of the initial value of S, the model trajectories are likely to remain in their original regime (LT or HT) for a number of years. This is an important result in the analogy to the climate system as it shows that reducing uncertainty in the measurement of a particular variable is only of value in climate prediction if the variable has an active role in the dynamic evolution of the system.

5.5.3 Convergence of IC ensembles

To quantify the memory of IC ensemble location in the LS84 model under passive coupling, KS comparisons between each pair of ensembles are presented for both ocean variables. Figure 5.17 shows the values of D over time for each of the six ensemble pairings. Focussing initially on T in figure 5.17(a), the results show that the ensemble pairing of *IC 1*/*IC 2* and the ensemble pairing of *IC 3*/*IC 4* converge more rapidly than the other ensemble pairings. This is because the ensembles originate in the same regime; ensembles *IC 1* and *IC 2* originate in the LT regime and ensembles *IC 3* and *IC 4* originate in the HT regime. The ensemble members spread initially in their regime of origin before transitioning to the other regime and spreading across the PA state space. After only 20 years the values of D approach a minimum for these two pairings.

The other KS comparisons show the rates of convergence in the ensemble distributions when the ensembles originate in different regimes. The rate of decline in D shows an exponential-like decay towards $D = 0$. The ensembles appear visually indistinguishable after approximately 180 years of the model simulation. The rates of convergence are nearly identical for the ensembles originating in different T regimes suggesting that the initial values of T strongly control the evolution of trajectories. Ensembles *IC 1* and *IC 3* are initially in different T regimes but their initial values of S are very similar. Nonetheless, these ensembles converge at the same rate as those ensembles with very different initial values in S.

The KS comparisons for the S variable in figure 5.17(b) support the conclusion that the rate of convergence is predominantly a function of the initial T values. Again, the two ensemble pairings that converge the fastest are ensembles *IC 1*/*IC 2*, and ensembles *IC 3*/*IC 4*. However, the rate of convergence is much slower because of the inertia of the system evident in the S variable. The values of D don't reach a minimum until at least 100 years of the model simulation have passed. The ensembles originating in different regimes converge even more slowly and D finally converges to a minimum after approximately 220 years. The initial decrease in D after 10 years for ensembles *IC 1*/*IC 3* occurs because the ensembles initiate with similar values of S but this decrease is premature as the values of T dominate the subsequent convergence.

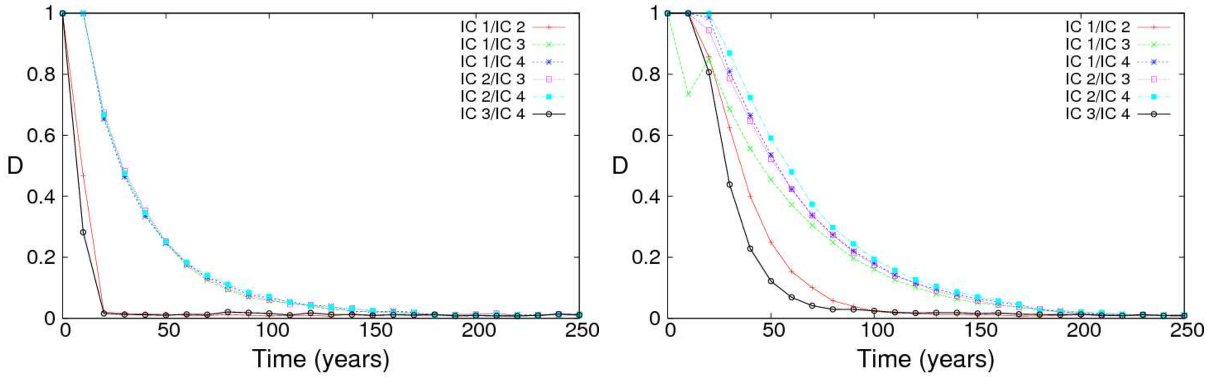

(a) T

(b) S

Figure 5.17: KS comparisons of the four IC ensembles shown in figure 5.14 for the T and S variables. Each line corresponds to the KS comparison for a different ensemble pair given in the figure key.

As described in section 5.2.3, the THC is temperature driven for the parameter values chosen. Under passive coupling, the initial values of T also strongly dictate the behaviour of the trajectories and the initial values of S appear to be unimportant in the evolution of the IC ensembles. In relating this work to the climate system, the results suggest that in order to improve predictions regarding the future evolution of variable climate distributions, it is important to constrain uncertainty in the dominant variables which control the system dynamics.

5.6 Climate Change in the LS84 Model

5.6.1 Rationale for experiments

In chapter four, the L84 model is used to investigate climate predictability when the model is forced from a region of parameter space associated with transitive behaviour to a region of parameter space associated with intransitive behaviour. In this section, the concept of climate under climate change is considered in the LS84 model which exhibits regime behaviour and almost intransitivity. Before proceeding it is important to re-examine the reasons for investigating climate change in this highly idealised coupled model. Given an increase in global atmospheric CO_2 concentrations, climate model projections largely agree about the direction and, to a lesser extent, magnitude of global and indeed regional changes in *mean* temperature (IPCC (2007b)). Yet there remains significant uncertainty in the nature of climatic changes at the regional scale with respect to extremes and tail events, in part due to the possibility of changing atmospheric and ocean dynamics. Circulation patterns which prevail under current forcing conditions may be very different under altered forcing conditions because of nonlinear responses in the climate system (Clegg et al. (2011)). Therefore, under changing global radiative forcing conditions, not only might we expect the mean of climate variable distributions to change at regional scales but also the shape of the variable distributions, reflecting altered dynamic behaviour of the climate system. Moreover, smooth transient changes in the radiative forcings do not imply that changes to climate distributions will also be smooth. Given the complexity of the climate system and the known existence of nonlinear system interactions, in the design-phase of climate model experiments it is therefore pertinent to consider the possibility of irregular and abrupt changes to the system's distributions. Given an appreciation of the complex nonlinear responses of the climate system to altered forcings, this section proceeds to explore the LS84 model under climate change.

In section 4.5 it is argued that the meridional temperature difference, represented by F, will decrease as the polar regions warm more rapidly than equatorial regions in response to anthropogenic radiative forcing. A trend towards lower values in F_0 is therefore imposed on the LS84 model to develop the analogy of the climate system under climate change. The focus of the LS84 model analogy is primarily on understanding the impact of almost-intransitivity on climate predictability and the memory of IC uncertainty in a system that evolves on more than one dynamic time scale. By introducing climate change into the LS84 model, the intention is to force the model between regions of parameter space which lead to alternative dynamic behaviour.

Considering the LS84 model under passive coupling is of more interest in the analogy to climate because of the existence of distinct regime behaviour (see section 5.2.4). However, Palmer (1999) asserts that the existence of regimes on decadal or longer time scales remains to be established. Suppose that the current climate is in fact largely transitive (i.e. regime behaviour, if present, is only found on short time scales). Now suppose that under a certain forcing scenario the climate is subject to almost intransitivity, leading to the onset of regime behaviour with relatively long residence periods. Such a change in the dynamic behaviour of the climate system under climate change may be possible at a regional and perhaps even a global scale but single climate model realisations are unlikely to be able to confirm or dismiss such conjecture. By performing experiments with the LS84 model subject to trends in the model parameters, the implications of such a change in the climate system dynamics for climate change prediction can be investigated.

5.6.2 Single trajectory results

In an idealised example, the LS84 model is forced from a region of parameter space associated with transitive behaviour to a region associated with almost intransitive behaviour (relative to the dynamic time scales of the system). Almost intransitive model behaviour representing a possible future climate scenario is given by the model under passive coupling parameters and a meridional temperature difference oscillating in the range $6 < F_0 < 8$ so that F_{0m} (mean F_0) is $F_{0m} = 7$. To establish an initial climate scenario which displays transitive behaviour, the LS84 model is run with a number of different values of F_{0m} under passive coupling and the resulting time series' in the ocean variables are analysed.

Figure 5.18 shows five single model trajectories of the model variable T for 1,000 year simulations of the LS84 model where F_{0m} takes values between $F_{0m} = 7$ and $F_{0m} = 9$. The model version used to generate figure 5.18(a) is therefore identical to that used to generate figure 5.4(b), albeit with a different initial state. Figure 5.18(a) therefore displays a similar trajectory evolution with abrupt transitions between the LT and HT regimes and relatively long residence times (decades to centuries) in each of the regimes. As F_{0m} is increased to $F_{0m} = 7.5$ (see fig. 5.18(b)), the distinct regimes disappear but a mode of long-term variability is still apparent in the time series, particularly evident between $t = 400$ and $t = 600$ years. In figures 5.18(c) to 5.18(e) the model trajectories show little evidence of centennial variability and appear to be dominated by more constrained short-term variability on annual, decadal and perhaps multi-decadal time scales. Relative to the model behaviour when $F_{0m} = 7$, the model appears largely transitive for values of $F_{0m} \geq 8$ shown in figures 5.18(c) to 5.18(e). Based on this evidence, a value of $F_{0m} = 8$ (where F_0 oscillates seasonally between $7 < F_0 < 9$) is chosen to represent the initial climate forcing.

In section 5.3.3 it is observed that when $F_{0m} = 7$ a single trajectory needs to be run a period of approximately 10,000 years before the ergodic assumption can be considered valid. The long simulation period is required because of the almost intransitive nature of the model in this region of parameter space dictated by the slow time scale in the model's ocean component. In the extended analogy presented in this section, the model is initially in a (relatively) transitive region of parameter space. The frequency distributions associated with three single trajectories, with slightly altered ICs, when $F_{0m} = 8$ are shown for the T variable in figure 5.19 after a 1,000 year simulation period (the distributions for S are given in Appendix C, figure C-5). The distribution listed as *IC 2* is associated with a trajectory initiated using the final state of the

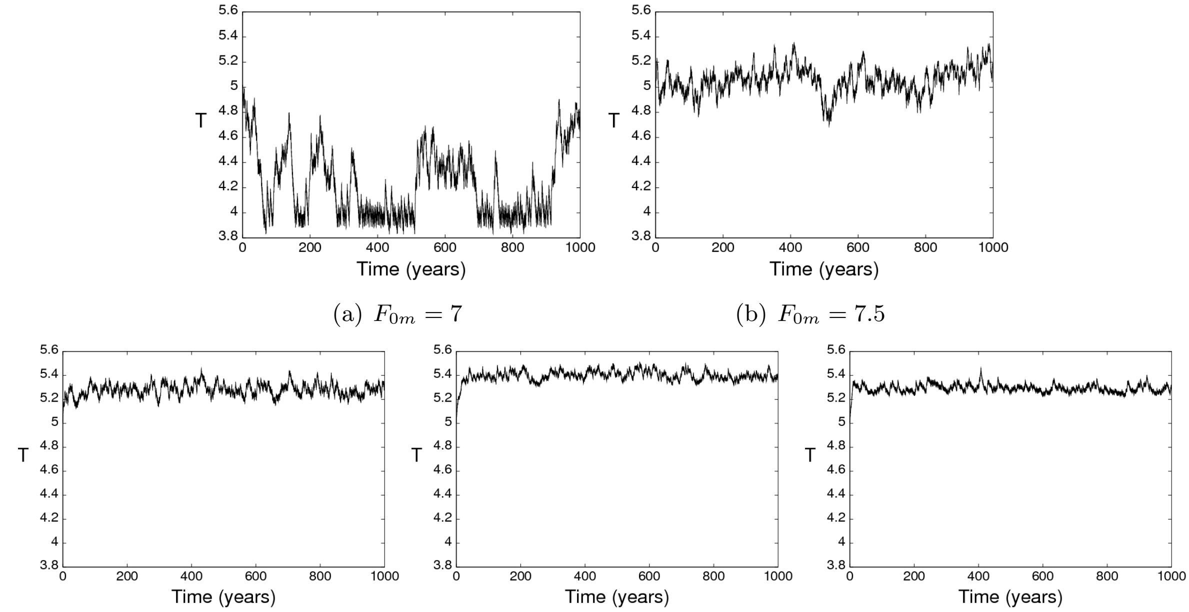

(a) $F_{0m} = 7$ (b) $F_{0m} = 7.5$

(c) $F_{0m} = 8$ (d) $F_{0m} = 8.5$ (e) $F_{0m} = 9$

Figure 5.18: Evolution of the LS84 model variable T with passive coupling for alternative values of F_{0m}. Each model simulation is initiated from the state $(X, Y, Z, T, S) = (1, 1, 1, 5, 1.5 \times 10^{-3})$.

trajectory shown in figure 5.18(c): $(0.167, 1.045, -0.547, 5.348, 1.352 \times 10^{-3})$. The other two single trajectory distributions are derived from model realisations initiated with ICs that are the same in all of the variables except T where the initial state is perturbed to $T = 5.248$ for *IC 1* and $T = 5.448$ for *IC 3*. There are some differences in the three distributions but they are all unimodal with peaks close to $T = 5.3$. The distribution for *IC 3* shows greater density in the high tail of the distribution. Each distribution serves as an approximation to the model climate for T when invoking the ergodic assumption. KS comparisons with a large IC ensemble climate distribution are provided later in this section.

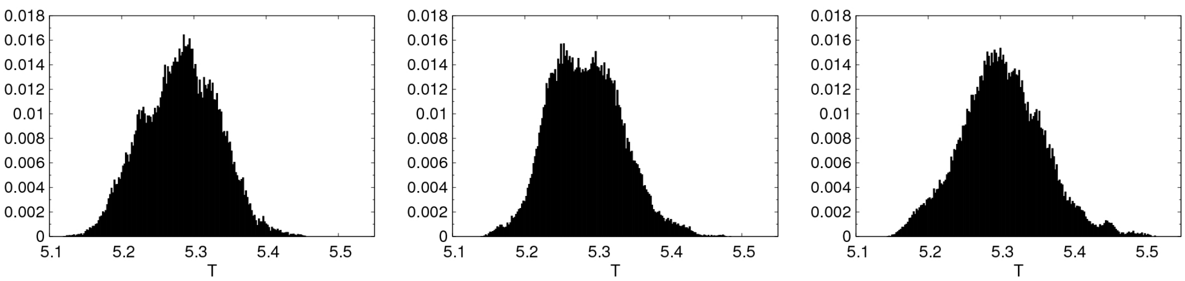

(a) IC 1 (b) IC 2 (c) IC 3

Figure 5.19: Normalised frequency distributions from three single trajectories of T from the LS84 model with passive coupling and a fixed value of $F_m = 8$, with different initial values in T. The three ICs correspond to: *IC 1* $= (0.167, 1.045, -0.547, 5.248, 1.352 \times 10^{-3})$; *IC 2* $= (0.167, 1.045, -0.547, 5.348, 1.352 \times 10^{-3})$; *IC 3* $= (0.167, 1.045, -0.547, 5.448, 1.352 \times 10^{-3})$. In each plot, the y-axis corresponds to the frequency of ensemble members per occupied bin; bin width = 0.002.

5.6.3 Single trajectory results under climate change

In the main experiment presented in this section, the model evolves according to a climate change scenario. The value of F_{0m} decreases linearly from $F_{0m} = 8$ to $F_{0m} = 7$ over the first 1,000 years of the simulation period according to equation 5.14 so that the rate of change in F_{0m} is equal to $\mu = -1 \times 10^{-3}$ (Kyr^{-1}). After 1,000 years, F_{0m} is then held constant at $F_{0m} = 7$ for the subsequent 1,000 years.

$$\frac{dF_{0m}}{dt} = \mu \tag{5.14}$$

Figure 5.20 shows the evolution of the T variable from three single trajectories with ICs used to generate the frequency distributions in figure 5.19 (for the S variable results, see Appendix C, fig. C-6). Even though the three trajectories are initiated with very similar ICs, the results show that the evolution of the trajectories over the 2,000 year simulation period are noticeably different. The divergence is not a particularly surprising result as the LS84 model displays chaotic behaviour in the parameter space explored in this experiment. More interestingly, the results show that the variability exhibited by the model trajectories is apparently dependent on the initial state. Focusing on figure 5.20(c), one might conclude by visual analysis of the time series that the final climate of the model is dominated by oscillations in the LT regime with occasional brief transitions to the HT regime. However, the responses of the model shown in figure 5.20(a) and in figure 5.20(b) display more transitions and longer residence periods in the HT regime. The underlying parameter conditions are exactly the same in each simulation so the differences in the variability that are observed are attributable to the initial state.

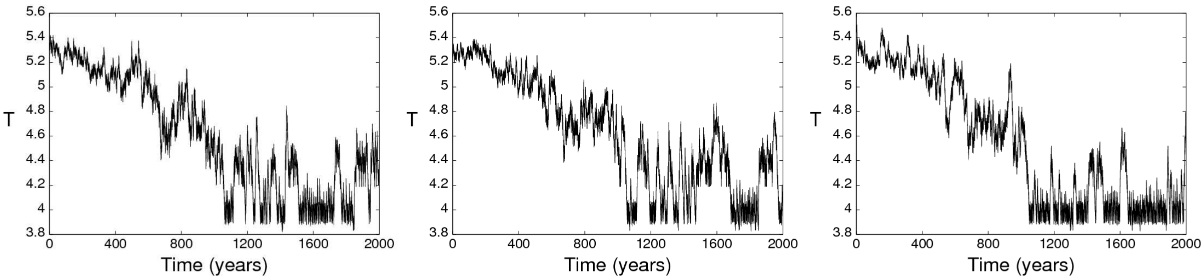

(a) IC 1 (b) IC 2 (c) IC 3

Figure 5.20: Evolution of three single trajectories of T from the LS84 model with passive coupling under climate change, with different initial values in T. The mean value of F decreases from $F_m = 8$ to $F_m = 7$ over the first 1,000 years and then remains constant at $F_m = 7$ for the following 1,000 years. The three ICs correspond to: *IC 1* = $(0.167, 1.045, -0.547, 5.248, 1.352 \times 10^{-3})$; *IC 2* = $(0.167, 1.045, -0.547, 5.348, 1.352 \times 10^{-3})$; *IC 3* = $(0.167, 1.045, -0.547, 5.448, 1.352 \times 10^{-3})$.

Figure 5.21 shows the frequency distributions associated with the last 1,000 years of the three model simulations illustrated in figure 5.20 (the corresponding distributions for S are shown in Appendix C, fig. C-7). The distributions highlight the differences observed in the single trajectory time series'. Figures 5.21(a) and 5.21(b) are visually similar with a small discrepancy in the density where $T \geq 4.6$. However, figure 5.21(c) shows considerably more density in the LT regime with a peak just below $T = 4.0$ that is almost double the magnitude of the corresponding peaks in figures 5.21(a) and 5.21(b). The increased residence time in the LT regime over the 1,000 year period is simply a consequence of the altered initial state. In the next section, IC ensemble distributions are determined and a quantitative comparison of the single trajectory distributions and the ensemble climate distributions is made using the KS test.

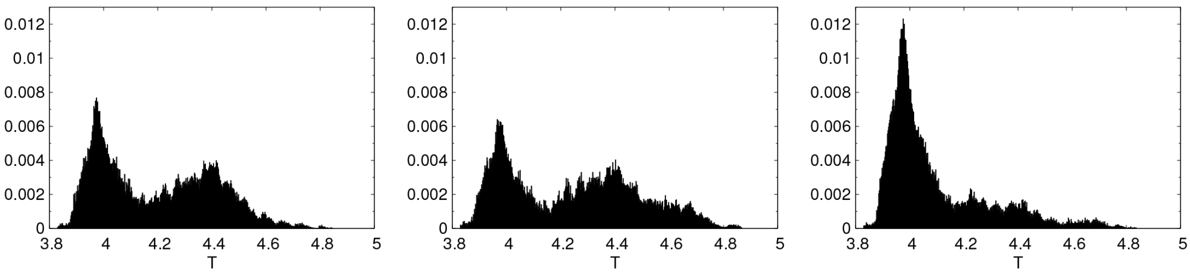

(a) IC 1 (b) IC 2 (c) IC 3

Figure 5.21: Normalised frequency distributions from three single trajectories of T from the LS84 model over a 1,000 year period following a linear change in F_{0m} from $F_m = 8$ to $F_m = 7$ over the previous 1,000 years (as in fig. 5.20). The three ICs correspond to: *IC 1* $= (0.167, 1.045, -0.547, 5.248, 1.352 \times 10^{-3})$; *IC 2* $= (0.167, 1.045, -0.547, 5.348, 1.352 \times 10^{-3})$; *IC 3* $= (0.167, 1.045, -0.547, 5.448, 1.352 \times 10^{-3})$. In each plot, the y-axis corresponds to the frequency of ensemble members per occupied bin; bin width = 0.002.

5.6.4 Ensemble results

A 10,000 member IC ensemble is used to estimate the climate distributions of the LS84 model for passive coupling when F_{0m} is initially fixed at $F_{0m} = 8$, and when F_{0m} decreases linearly toward $F_{0m} = 7$ as described in sections 5.6.2 and 5.6.3 respectively. The IC ensemble consists of 10,000 members, each of which have the same initial value of X, Y, Z and S whilst the initial value of T is given for evenly spaced increments in the range $5.248 < T < 5.448$ to match the range explored for the three individual model realisations.

The 3D colour-maps in figure 5.22 show the evolution of the ensemble over a 1,000 year simulation period when $F_{0m} = 8$. Figure 5.22(a) shows that the range in T is well explored after 100 years with the majority of ensemble members located in the region $5.2 < T < 5.4$. The specific details of the distribution changes subtly at each time instant but the broad characteristics remain consistent over the duration of the model simulation. Similarly figure 5.22(b) shows that the distributions in the S variable are well explored after 100 years with the majority of members in the range $1.34 < S < 1.37 \times 10^{-3}$.

Figure 5.23 shows the KS comparison between the ensemble distributions at each 100 year interval (at mid-winter every 100 years) and the ensemble after the 1,000 year simulation period for the T and S variables; hence $D = 0$ at $t = 1,000$. The value of D approaches $D = 0$ in both variables for all time instants where $t > 0$ years indicating that the ensemble has converged.

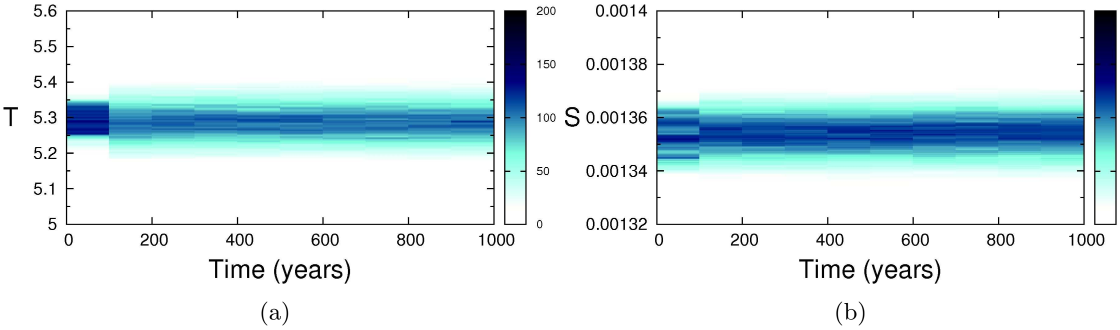

Figure 5.22: 3D colour-map showing the evolution of a 10,000 member IC ensemble in the passively coupled LS84 model when $F_{0m} = 8$ for the variables T and S. The ensemble members have ICs: $(0.167, 1.045, -0.547, T, 1.352 \times 10^{-3})$ where T is uniformly distributed in the range $5.248 < T < 5.448$.

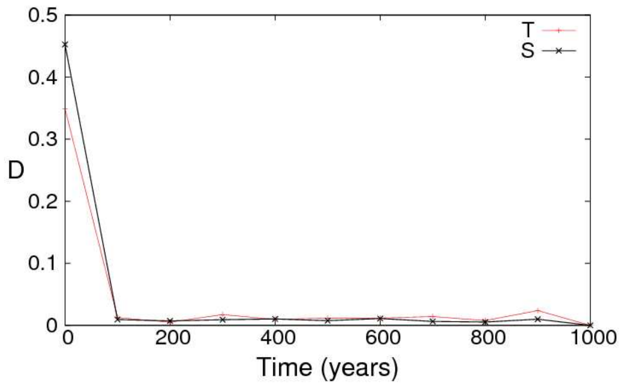

Figure 5.23: KS comparison for the T and S variables between the IC ensemble distributions after a 1,000 year simulation and the evolving ensemble distributions at 100 yearly intervals over the 1,000 year simulation period.

The values of D are between $0.005 < D < 0.024$ for both T and S where $t \geq 100$ years.

The KS test is also used to compare the single trajectory frequency distributions shown in section 5.6.2 to the ensemble distributions after the 1,000 year simulation period. The values of D are given in table 5.5. In both variables, the values of D are higher than the values associated with IC ensemble distributions. This shows that a 1,000 year simulation period of a single trajectory is insufficient to assume ergodicity in the LS84 model when $F_{0m} = 8$. Furthermore, the distributions are less similar in the S variable than in the T variable where the values of D are closer to $D = 0$ due to the inertia in the ocean salinity noted previously. The KS comparison therefore provides a measure of reliability for the ergodic assumption quantifying the ability of single trajectories to produce climate statistics that approximate the climate statistics of the ensemble climate distributions associated with the underlying PA.

Figure 5.24 shows the evolution of the same 10,000 member ensemble when subject to a decreasing trend in F_{0m}, described in section 5.6.3. The ensemble distribution is initially well

Variable	*IC 1*	*IC 2*	*IC 3*
T	0.0579	0.0577	0.0908
S	0.1553	0.1181	0.1137

Table 5.5: KS comparison for the T and S variables between the IC ensemble distributions illustrated in figure 5.22 after a 1,000 year simulation and the single trajectory distributions given in figures 5.19 and C-5 when $F_{0m} = 8$.

constrained in both the T and the S variables and over time the values of T decrease and the values of S increase whilst the range in the distribution expands. After 600 years, there appears to be a small step-change present where trajectories temporarily evolve on a PA where $T \approx 4.8$ and $S \approx 1.5 \times 10^{-3}$. After 1,000 years the trend in the F_{0m} ceases and a larger step-change is evident as the ensemble distributions move rapidly towards the climate distributions associated with the model PA at $F_{0m} = 7$. The ensemble distributions provide the range and relative likelihood of possible states conditioned on the IC uncertainty (embedded in the ensemble design).

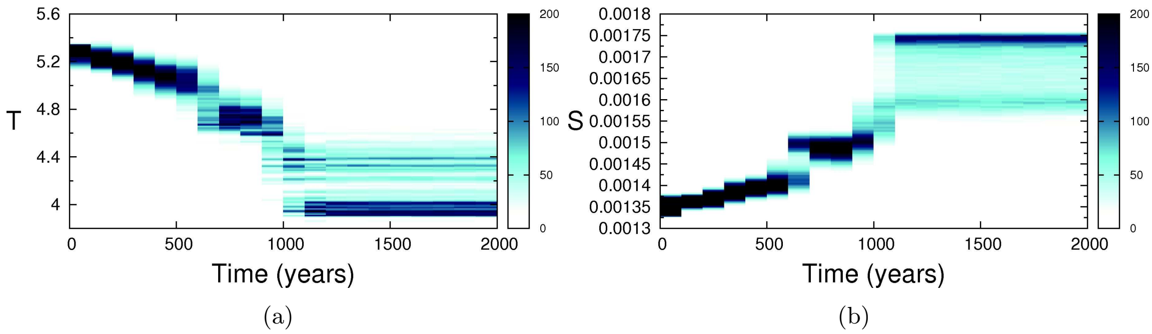

Figure 5.24: 3D colour-map showing the evolution of a 10,000 member IC ensemble in the passively coupled LS84 model for the variables T and S when $F_{0m} = 8$ initially and then linearly decreases to $F_{0m} = 7$ after 1,000 years and is then held constant. The ensemble members have ICs: $(0.167, 1.045, -0.547, T, 1.352 \times 10^{-3})$ where T is uniformly distributed in the range $5.248 < T < 5.448$.

The single trajectory distributions shown in figure 5.21 are compared to the IC ensemble distributions after the 2,000 year simulation period using the KS test. The results are presented in table 5.6. For *IC 1* and *IC 2*, the values of D increase slightly in the T variable compared to the values derived when $F_{0m} = 8$, given in table 5.5. For *IC 3*, the value of D increases dramatically. A similar result is also observed in the S variable. The results show that the use of the ergodic assumption for a 1,000 year simulation period becomes slightly less reliable for *IC 1* in the T variable and for both T and S in *IC 2* under transient parameter conditions. The ergodic assumption appears to be significantly less reliable for *IC 3* in the climate change scenario presented. In this experiment only three single model realisations are investigated so any conclusion regarding the applicability of the ergodic assumption under climate change in the LS84 model is necessarily tentative. Nonetheless, the results imply that confidence in the ability of a single model realisation to provide reliable quantitative information regarding the climate distributions of the LS84 model under one set of parameter conditions need not necessarily lead to confidence under altered parameter conditions; further single model runs would be beneficial in refining the conclusion for the LS84 model. More importantly the experiment provides a methodological approach for assessing the reliability of the ergodic assumption for the studies of the climate system involving more complex climate models.

Variable	*IC 1*	*IC 2*	*IC 3*
T	0.0683	0.0884	0.2458
S	0.1242	0.1643	0.3040

Table 5.6: KS comparison for the T and S variables between the IC ensemble distributions illustrated in figure 5.24 after a 2,000 year simulation and the single trajectory distributions given in figures 5.21 and 5.21 when F_{0m} is stabilised at $F_{0m} = 7$ after a 1,000 year linear trend from $F_{0m} = 8$ to $F_{0m} = 7$.

In section 5.3.3 it is shown that a single trajectory frequency distribution, derived from a simulation period of hundreds or even thousands of years (under passive coupling), provides misleading information about the PDFs associated with the PA of the LS84 model under passive coupling, even in the absence of trends in the parameters. In this section, the methodology developed could help to explore whether or not the level of confidence in the ergodic assumption resulting from analysis under particular parameter/forcing conditions is misplaced when extrapolating to the behaviour of the model under altered parameter/forcing conditions. Increasing the scope and scale of the experiment presented here would help to refine the conclusions in the context of the LS84 model. However, potentially more value could be gained by following the methodology to study a range of more complex climate models which exhibit variability on a number of time scales due to the inclusion of more climatic processes. Further discussion of the implications for model experimental design is given in section 5.7.

5.7 Discussion of LS84 Results

5.7.1 Climate variability in a simple coupled model

The climate system includes many subsystems for which the initial state is poorly known. In using simple nonlinear models to inform the design of GCM experiments, it is sensible to focus on the interaction of the primary components which control the variables of interest, on the time scales of interest. The ocean and the atmosphere operate on different time scales and the ocean plays a critical role in determining atmospheric circulation patterns. The ocean also affects the timing and magnitude of extreme events, such as the development of hurricanes and tropical storms which are of particular interest to insurers, so understanding modes of variability in the ocean is a crucial element of the climate change prediction problem.

In section 5.2.5 it is shown that the dynamics of the ocean component of the LS84 model play a significant role in determining the behaviour of the atmosphere. The state of the ocean influences the annual variability in the atmosphere and appears to control the number of summers in which atmospheric variables evolve towards a fixed point solution. The chapter therefore focuses on the role of IC uncertainty in the ocean.

To develop an understanding of climate under climate change and improve predictive capabilities on the time scales of interest to policymakers, it is essential to account for internal climate variability. In the LS84 model, long-term internal variability is manifest in regime behaviour present in the ocean variables, when the model is subject to passive coupling. The internal variability occurs on centennial time scales and the regimes are distinct (in the T variable) leading to almost intransitivity. Lorenz (1997) states that it is difficult to establish whether or not the climate system is indeed almost intransitive but Lorenz explains that "almost intransitivity implies the existence of two or more time scales, which the climate system certainly possesses".

5.7.2 Utilising IC ensembles

Because of the presence of long-term variability in the LS84 model, the use of single model realisations to estimate the model climate PDFs is limited. The ergodicity of the LS84 model is investigated in section 5.3.3 and the results show that almost intransitive behaviour restricts the applicability of the ergodic assumption, even in the absence of trends in the model parameters. The possible existence of almost intransitive behaviour in the climate system (on any relevant spatial and temporal scale) means that an externally driven climate change may be indistinguishable from an internally driven climate change given only one time series of observations. This not only has important implications for the attribution of past climatic changes (as noted by Lorenz (1991a)) but also for how climate models are used to project future climate change and how model output is interpreted by users.

In section 5.4, the LS84 model is used to help determine an appropriate IC ensemble size to provide robust quantitative probabilistic information about the model climate distributions. An experiment is conducted to determine the minimum ensemble size required to produce a reliable estimate of the probability of a trajectory being in a given regime after a specified simulation period. The results suggest that an ensemble size of 2,000 to 4,000 members is sufficient but any fewer isn't. The experiment is also inverted to determine the memory (traceability of IC uncertainty) in the LS84 model by plotting the percentage of ensemble members (from an IC ensemble originating in the LT regime) in each regime at various time instants, for fixed ensemble sizes. The results show that memory of the IC ensemble is present for a period of up to 200 years. The implication is that multi-decadal and/or centennial variability in the climate system might cause the distributions of climate variables to be IC dependent for many decades or even hundreds of years.

5.7.3 Memory of ICs in the LS84 model

Whilst the memory of ICs in the atmosphere may be lost over a number of weeks, the memory that resides in the oceans and other subsystems of the Earth's climate system (such as the cryosphere, biosphere or stratosphere) is relevant on much longer time scales. As noted by Ghil (2001), "the interactions between the subsystems give rise to climate variability on all time scales". How the memory of ICs in the slowly evolving subsystems influence the evolution of the climate system under altered forcings is highly uncertain. How internal variability reacts under transient forcing is complicated further still (Epstein and McCarthy (2004)).

The time it takes for an ensemble to converge to the model climate distributions provides a measure of the memory of ICs in the model. The evolution of IC ensembles from a transect across the PA state space is presented in section 5.3.2 and the rate at which the ensembles explore the range of model states consistent with the models PA is found to be different for active and passive coupling. Because the model exhibits long-term centennial variability under passive coupling, there is a greater memory of the ensemble ICs and a longer model simulation is required before the IC ensemble approaches the model climate distributions.

Experiments relating to the convergence of model ensembles from different locations on the PA under passive coupling are presented in section 5.5. The convergence between IC ensembles is shown to be dominated by the initial values of T. IC ensembles from the same initial regime converge rapidly but IC ensembles from different regimes converge more slowly. This is an important result in the analogy to the climate system as it means that long-term modes of variability affect the spread of IC uncertainty. Moreover, the results show that reducing uncertainty in the measurement of a particular system variable may reduce the spread in uncertainty for future climate states but only if the variable has an active role in the dynamic evolution of the system.

5.7.4 LS84 with climate change

In section 5.6, the behaviour of LS84 model is investigated when subject to a trend in F_{0m} moving the model between a region of parameter space considered largely transitive to a region which is almost intransitive under passive coupling. The results of single model trajectories are displayed, showing that the evolution of the model is sensitive to ICs. Observing the model behaviour over a simulation period of 2,000 years reveals that the variability exhibited by the model trajectories under altered parameter conditions is dependent on the initial state of the model. The methodology used in the main experiment examines the reliability of the ergodic assumption and in the LS84 model, albeit with a limited sample of single model realisations, the tentative conclusion is that changes in the dynamic behaviour associated with the model parameter conditions limit the reliability of the ergodic assumption. Confidence in estimating the distribution of past climates from a single trajectory need not necessarily lead to confidence in the ability of single trajectories to capture the range of states consistent with some future forcing scenario. Further experiments with more model runs analysing the behaviour of the model in different regions of parameter space would be valuable to understand how the dynamic interactions affect the validity of the ergodic assumption. Furthermore, the methodology could be applied to more complex climate models to understand the implications for assuming ergodicity in the climate system which displays variability on a number of different time scales.

5.7.5 Value of the LS84 model experiments

In the next chapter, the focus is directed towards the use of climate model information in the insurance industry. Addressing the needs of the user community whilst ensuring that scientific uncertainties are well explored is a significant challenge given limited computational capacity. Nonetheless, the results and discussion presented in chapter six suggest that user demands and scientific rigour can be consolidated by the appropriate design of climate model experiments. The objective of the experiments conducted with the LS84 model, and indeed the L63 and L84 models, has therefore been to gain insight into the complex dynamic behaviour of a nonlinear system analogous to the climate system, to guide the design of climate model experiments.

The results presented in this chapter have implications for the way climate modellers explore and interpret uncertainty using GCMs. The seasonally driven LS84 model has been explored to highlight the dangers of relying on the ergodic assumption for a system which displays long-term variability and almost intransitive behaviour. Large IC ensembles are necessary to estimate the climate of the model under fixed and altered parameter conditions and to explore the range of possible states consistent with the IC uncertainty. Ultimately, for climate model experiments to be useful to the user community, they ought to explore all possible future scenarios. This requires a thorough exploration of epistemic and aleatoric uncertainty. Establishing what is possible is a precursor to determining what is likely.